IEEE Access
Multidisciplinary : Rapid Review : Open Access Journal

Received August 23, 2016, accepted September 28, 2016, date of publication October 19, 2016, date of current version November 18, 2016.

Digital Object Identifier 10.1109/ACCESS.2016.2618905

A Unified Routing Framework for Integrated Space/Air Information Networks

WEIJING QI[1], WEIGANG HOU[1], LEI GUO[1], (Member, IEEE), QINGYANG SONG[1], (Senior Member, IEEE), AND ABBAS JAMALIPOUR[2], (Fellow, IEEE)
[1]School of Computer Science and Engineering, Northeastern University, Shenyang 110819, China
[2]School of Electrical and Information Engineering, University of Sydney, Sydney, NSW 2006, Australia

Corresponding author: L. Guo (guolei@cse.neu.edu.cn)

This work was supported in part by the National Natural Science Foundation of Major Research Project in China under Grant 91438110, in part by the National Natural Science Foundation of China under Grant 61401082, Grant 61471109, and Grant 61303250, in part by the Fundamental Research Funds for the Central Universities under Grant N130817002, Grant N140405005, and Grant N150401002, and in part by the Foundation of the Education Department of Liaoning Province under Grant L2014089.

ABSTRACT The aerospace-based communications can be managed more efficiently through the construction of an integrated space/air information network by the convergence of satellite (space) and unmanned aerial vehicle (air) networks. Such an integrated network would best fit the advent of delay- and disruption-tolerant networking, in which the data transmission can tolerate long delay and disruption under a store-carry-forward mechanism. Such a network, however, has some challenging research needs due to the network's high mobility of nodes and time-varying topology that may result in high error bit rate and long delay. In this paper, we propose a unified routing framework for this integrated network, where a Hybrid time-space Graph supporting Hierarchical Routing (HGHR) algorithm is achieved. More specifically, the HGHR performs on a hybrid time-space graph, including two subgraphs: a deterministic graph for the space network and a semi-deterministic one for the air network. This latter graph is based on a discrete time homogeneous semi-Markov prediction model. The hybrid time-space graph is then transformed into a state-space graph, based on which, a message forwarding rule under the store-carry-forward mechanism is adopted. Simulation results show that the proposed HGHR algorithm has good performance in terms of message delivery ratio, end-to-end delay, and power consumption.

INDEX TERMS Routing, integrated space/air information network, hybrid time-space graph, semi-Markov prediction model.

I. INTRODUCTION

Over the past decades, satellite systems, for their wide coverage and broaden applications, have been rapidly developed along with the significant investment from governments and enterprises into the aerospace field. However, these variety of satellites always run independently since their communication protocols have not been unified, which results in a series of problems. Take an example in the domination of Earth observation, as shown in Fig. 1, the link labeled by 1 between a high-orbit satellite and a ground station is unreliable, which may lead to observational data loss. While for a low-orbit satellite moving with data, as labeled by 2, the communication window only lasts for a few minutes, posing a major challenge to the data transmission rate of space sensors. To overcome these obstacles, satellite networks, where Inter-Satellite Links (ISLs) labeled by 3 in Fig. 1 are supported, have been attracting significant attention in the areas of communication, remote sensing and global positioning. Despite the provision of large coverage, the distant and expensive satellites usually bring large cost especially for some local-scale services. To address this issue, National Aeronautics and Space Administration (NASA), Defense Advanced Research Projects Agency (DARPA) and some other organizations have made significant efforts on developing civil uses of Unmanned Aerial Vehicles (UAVs) in the last decade [1], showing the possibility of UAVs acting as an attractive complement to satellite systems for strengthening regional communication or observation services. Since the payload of a UAV is limited, a network with multiple UAVs labeled by 4 in Fig. 1 is dominant for enhancing scalability.

Recently, the need to make full use of satellite/UAV resources has stimulated active research efforts on

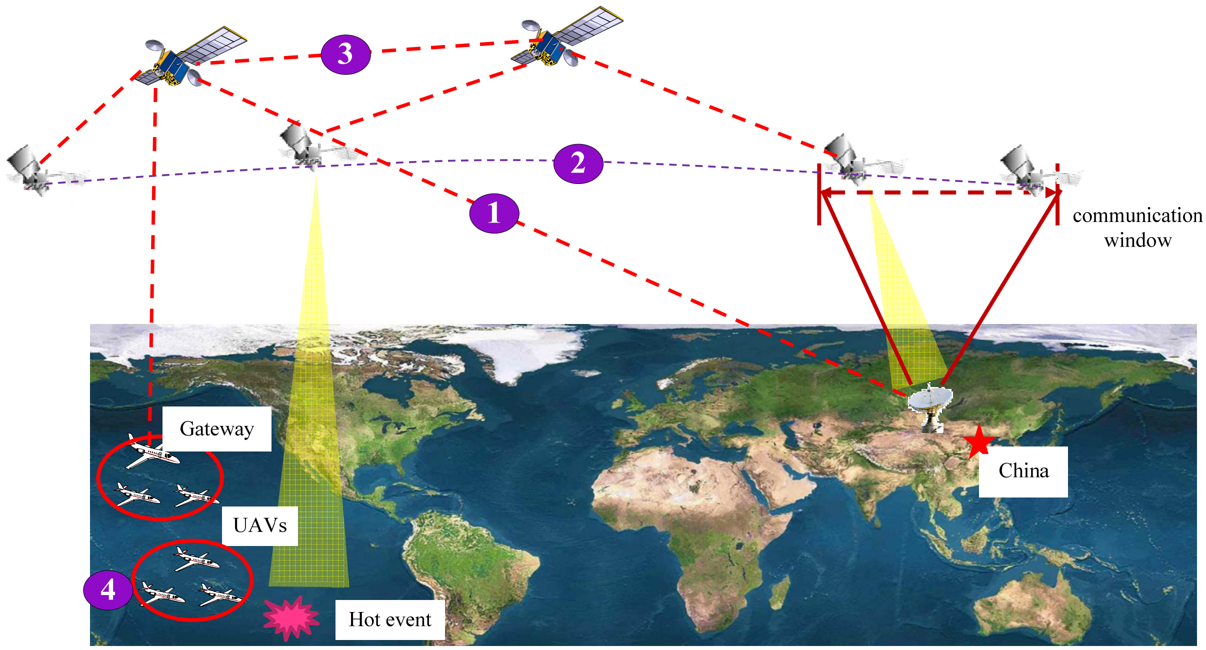

FIGURE 1. Illustration of 4 transmission methods by space/air resources. 1: relay data by a long satellite-ground link when the ground station is within the satellite's coverage, but the link is always unreliable. 2: carry data by a satellite and transfer to the ground station in the communication window, while the delay is very long. 3: transfer data by space network which could compensate 1 and 2. 4: the air network composed by air-marks could strengthen regional communication and a UAV gateway is selected to communicate with satellites.

constructing an integrated space/air information network so that it could provide high-quality services on a large scale with low cost. Fig. 2 shows the architecture of an integrated network. Due to the load limits, only a certain number of UAVs equipped with hardware could act as gateways, which are responsible for communicating with satellites. The air region is partitioned as some sub-regions called air-marks. Each UAV continuously maintains inter-air-mark flying regularly, and contacts could be established between UAV pairs only belonging to the same air-mark, with ad hoc networking being applied in the air network [2]. As defined in [3], the contact here means that two nodes establish a communication link successfully so that they can exchange data directly.

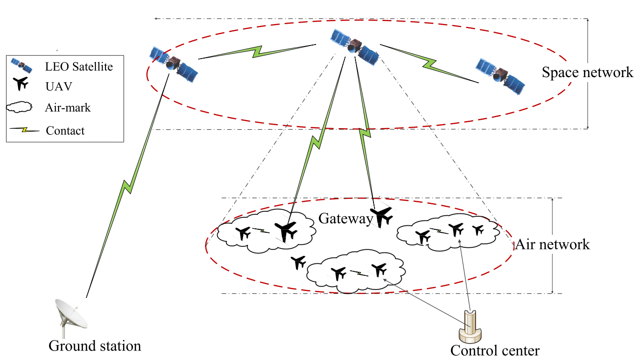

FIGURE 2. Example of an integrated space/air information network. With limited number of UAV gateways which could communicate with satellites, there are two ways for inter-UAV communications: UAVs move as ferries; UAV gateways and satellites act as data relays.

Since this integrated network is a stereo-network with heterogeneous nodes and links in harsh space/air environments, the research of efficient routing protocols is complicated and challenging. More specifically, it bring the following challenges:

(i) *Universal protocol architecture.* The research on Delay- and Disruption- Tolerant Networking (DTN) [4] architecture, which introduces a global overlay above the transport layer–Bundle layer, becomes active recently. Thanks to the store-carry-forward mechanism provided by the Bundle protocol, two basic benefits are obtained: communications among heterogeneous networks with diverse protocols could be realized and path selection for bundles is necessary in the Bundle layer; each node under the DTN architecture can store data for a long time before forwarding, which is suitable for networks characterized by long delay and disruption. The integrated space-air information network would best fit the DTN architecture. For the case that source and destination UAVs are in different air-marks, communications will be achieved via UAVs moving among air-marks which act as "data mules" for message ferrying incidentally, or through UAV gateway and satellite relays as an alternative. However, the existing DTN routing algorithms have been mainly designed for space or air networks separately, and there has been little study on the unified routing protocol in the integrated information network.

(ii) *Topology characterization*. Early routing protocols proposed for satellite networks took the deterministic network as a long series of snapshots, transforming the dynamic routing problem into a static one [5]. Recently, the time-varying topology characterization [6], [7] is proposed. Furthermore, time-space graph models including both spatial and temporal information have been applied [8] in DTN networks. Nevertheless, most of the previous topology graphs aimed to model a single deterministic network, but little try for an integrated network with deterministic and also predictable subnetworks.

(iii) *Prediction for node movement*. To improve the routing performance in terms of message delivery ratio and end-to-end delay in DTN networks with short-lived wireless connectivity, the prediction of node location or link quality is quite necessary. Many studies on prediction models which take advantage of nodes' historical moving data have been done, mainly including Markov model [9], spatiotemporal correlation model [10], gray prediction model [11], and data mining model [12]. Unfortunately, little prediction model predicted the contact time between nodes which is a significant factor in DTNs.

To solve the above challenges on routing design in the integrated space/air information network, the strategy of "divide and conquer" and also "combine and integrate" are utilized in our proposed unified routing framework, based on which, a Hybrid time-space Graph supporting Hierarchical Routing (HGHR) algorithm is achieved. More specifically, HGHR performs on a hybrid time-space graph which contains two subgraphs: a deterministic one for the space network and a semi-deterministic one for the air network. Among them, to build the semi-deterministic subgraph, we introduce a semi-Markov model for prediction of contact time and contact probability between all UAV pairs. Next, the hybrid time-space graph is transformed into a state-space one, based on which, a message forwarding rule is proposed under the store-carry-forward mechanism. The key contributions are listed as follows:

- We proposed a prediction model, in order to predict contact time and contact probability between all UAV pairs with a high prediction accuracy. Based on the prediction results, each UAV obtained sufficient topology information so that appropriate routes could be decided, increasing message delivery ratio and decreasing end-to-end delay.
- We constructed a hybrid time-space graph that contained a deterministic time-space subgraph for the space network and a semi-deterministic time-space subgraph for the air network. The two networks could be thus efficiently integrated into a whole one for topology characterization.
- According to the contact time and contact probability, we designed a message forwarding rule to select an optimal next hop in the hybrid graph, taking UAVs or satellites as relays.

The following paper is organized as follows. An overview of routing in DTN networks is described in Section II. In Section III, we review the related works concerning DTN routing. A unified network framework for the integrated space/air information network is introduced in Section IV. Our discrete time-homogeneous semi-Markov model is built in Section V. In Section VI, a hybrid time-space graph model is constructed, and we propose the HGHR algorithm for the integrated information network in Section VII. Simulation results are shown in Section VIII before conclusion and prospect of future work in Section IX.

II. ROUTING IN DTN NETWORKS

By traditional definition, routing is the procedure by which we select the best path for transmitting data from a source node to a destination node in a network, where the measurement is some simple metric (e.g. the number of hops). In TCP/IP networks, the end-to-end path is guaranteed by the transport layer of the source node, based on the network topology information that is a list of nodes and links. However, as mentioned above, the integrated space/air information network is a DTN network supporting asynchronous communications. What makes it different from traditional terrestrial networks is the frequent link interruption and rapid node movement. The link information such as the capacity and duration of each contact becomes important. Hence the traditional methods used for computing routes in terrestrial networks are not suitable for a DTN network.

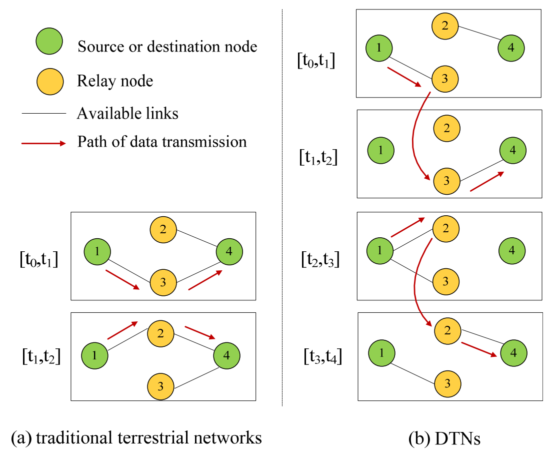

FIGURE 3. Comparison of data forwarding in different networks. (a) data forwarding in traditional terrestrial networks. There are complete paths in the topology across a sequence of time slots. (b) data forwarding in DTN networks. Data need to be stored in some nodes for a period of time since there is no complete path in the following sequence of time slots.

Specifically, in dynamic networks, the network state information is changing over time, and therefore the most efficient route may change. The duration that the topology remains static is usually enough for a data transmission process, in spite of the topology variation. As shown in Fig. 3 (a), when node 1 sends data to node 4, there are two complete paths separately in the period of $[t_0, t_1]$ and $[t_1, t_2]$: $1-3-4$ and $1-2-4$. Therefore, the data needn't wait in a certain node.

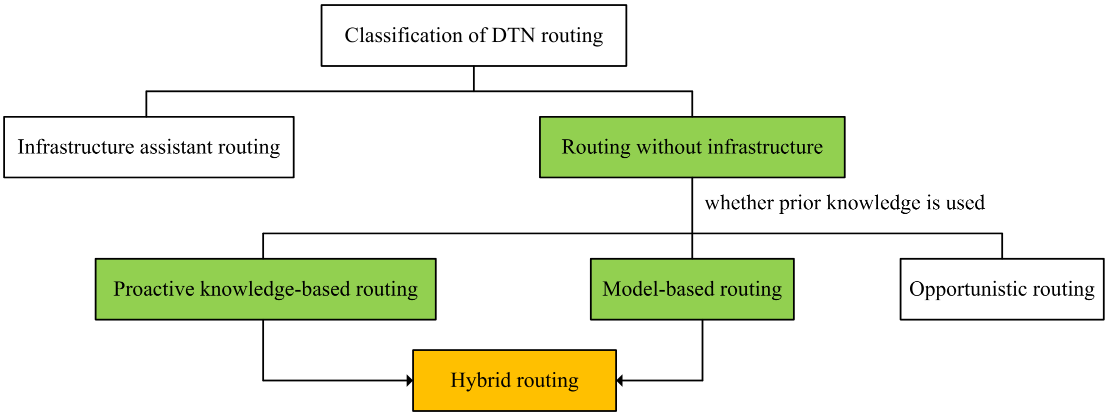

FIGURE 4. Classification of existing DTN routing. The work of this paper belongs to the category of routing without infrastructures, Below which, the proactive knowledge-based routing is suitable for those networks where the movement information of nodes is known in advance. The model-based routing is suitable for some other networks where the movement information can be predicted. A new hybrid routing combining the knowledge- and model- based routing is adopted here.

In a DTN network such as the integrated space/air information network in our paper, this is not true. Since its connectivity is intermittent, network state changes faster than being updated in each node [13], [14]. During a data transmission process in DTN networks, there may be no complete path to the destination. As shown in Fig. 3 (b), the connections between nodes are intermittent in four periods of $[t_0, t_1]$, $[t_1, t_2]$, $[t_2, t_3]$ and $[t_3, t_4]$. If node 1 wants to send data to node 4, no complete path can be found in any single period. Hence the most desirable objective of DTN routing is not to minimize delay but to improve message delivery. Certainly, only when the delay is within the time-to-live, the message can be delivered successfully. Routing in DTN networks becomes a matter of choosing a neighboring node as a next-hop to get closer to the destination. The store-carry-forward mechanism is supportive to this. The source node transmits a message to its neighboring node and asks it to take custody. Once the neighboring node accepts custody, the original node will no longer responsible for the message and the node taking the message is entitled for forwarding. In Fig. 3 (b), node 1 first sends data to node 3 in $[t_0, t_1]$, then node 3 takes custody and transfers data to node 4 in $[t_1, t_2]$. We can see that the data transmission is not continuous but waits for a period of time in node 3. Therefore, prior plans or predictions on topology changes become important and the time-space graphs become necessary for deciding a path in DTN networks..

III. SURVEY OF CURRENT WORK

As mentioned above, the unified routing in the integrated space/air information network are mostly designed under the DTN architecture. Since K. Fall proposed the concept of DTN [4] in 2003, numerous works were done on DTN routing. The classification of existing DTN routing is shown in Fig. 4. The work of this paper belongs to the class of routing without infrastructures. Considering the characteristics of the integrated space/air network, we propose new hybrid routing mechanism combining the knowledge- and model-based routing. In this section, we summarize the existing works in these three aspects and also routing in heterogeneous networks.

A. PROACTIVE KNOWLEDGE-BASED ROUTING

In proactive knowledge-based routing, routes are computed for an overall topology graph before traffic arrivals. Jain et al. explained the knowledge as contacts, queueing and traffic demand in [15]. In an intermittent DTN network, nodes always fail to request a full path to the destination in a traditional static graph. Many works have been done on novel topology characterizations. For example in [16], the authors utilized topology snapshot sequences maintained in each node to record the changing process of the network topology. In [17], the authors constructed a deterministic time-space graph for satellite backbone networks, by which, the optimal path for any node pair could be determined. also Caini et al. also address space network use case in [18]. The authors in [8] also constructed a deterministic time-space graph model. Considering the unreliability of network links, an appropriate threshold of link reliability was set to reduce the topological cost by deleting unreliable links.

A recently proposed Contact Graph Routing (CGR) [19] for networks with perfect knowledge becomes a research hot spot [20]. The basic idea is that each node holds a contact list for every possible destination node and then a successive contact sequence backward from the destination node, which is taken as a route, can be obtained. In 2011, Jet Propulsion Laboratory (JPL) proposed two improvements for enhancing CGR for space networks [21]: using path weight by earliest arrival time rather than forfeit time; using Dijkstraąŕs shortest path algorithm for path selection, thus guaranteeing CGR free of routing loops and persistent oscillation.

However, the above mentioned routing schemes only work with perfect knowledge, which is often not available in practice.

B. MODEL-BASED ROUTING

In real DTN scenarios, if no plans are obtained, prior knowledge is difficult to be discovered via dialogue due to the intermittence. Fortunately, the node mobility is always being highly predictable and amenable to simplified models such as social models or mobile models. Many researchers have explored extensively research on the DTN routing based on network models. Leguay et al. [22] once proposed a generic routing scheme based on a high-dimensional Euclidean space model constructed upon historic information. It had been shown in a real scenario that the proposed routing scheme brings benefits in terms of bundle delay and communication cost.

An association-based contact prediction model with high accuracy was proposed in [24]. Based on the contact prediction, a routing scheme called Plankton was designed to control replicas by contact probability and message delivery probability, greatly reducing network overhead while maintaining stable delivery ratio and end-to-end delay. Furthermore, a Markov prediction model was proposed in [25], where possible locations of an arbitrary target node were predicted by the second-order Markov prediction mechanism. It effectively improved the packet delivery ratio and reduced the network overhead. Besides, Kalman filters [26] and data mining models [27] were also be utilized as prediction models to improve the routing performance.

Most works studied models for prediction of contact or node trajectory using historical information in semi-deterministic DTN networks. However, little work considers constructing a network graph based on the prediction results, which could transform the dynamic routing problem into a static one.

C. OPPORTUNISTIC ROUTING

For some opportunistic DTN networks, the node mobility is unpredictable and the paths to destinations are difficult to decide. The Direct Transmission [28] and Epidemic Routing [29] were most widely used. The former one claimed that the source node would not forward data to any relay unless it encountered the destination node, thus saving network overhead but at the cost of long delay. In the Epidemic Routing, no routing decisions are done and each node keep flooding data copies to any nodes it encountered until one of the copies arrived at the destination node, which absolutely results in a huge waste of resources.

For the two extreme cases, many researchers proposed a number of heuristic algorithms, aiming to improve the routing performance and minimize the resource overhead. For example, Diana et al. [30] designed a DTN routing algorithm which controlled the optimal number of data copies to minimize the resource consumption under an acceptable delay for quasi-deterministic networks. Using the idea of ąřEmployee mechanismąś, Erramilli et al. [31] proposed a delegation forwarding routing algorithm where the number of message copies is limited, achieving the same effect. The Probabilistic Routing Protocol using History of Encounters and Transitivity (PROPHET) [32] is based on probability estimation. Each node would estimate its P-value, that is the probability of arriving at the given destination, based on their historical contact frequency.

D. ROUTING IN HETEROGENEOUS NETWORK

In many real communication scenarios, heterogeneous networks with more than one mobility pattern may happen. The routing problem hence may be more complicated. The authors in [33] addressed the routing problem in DTN networks comprising multiple classes of nodes with diverse characteristics and mobility patterns. They proposed a scheme using a fixed number of copies, in order to control resource usage and achieve the best possible performance. A gateway-based inter-domain routing scheme for DTN networks is proposed in [34]. A gateway node was selected in each domain from some candidates dynamically, which could reach foreign domains. Besides, for air networks, Lee et al. [35] presented a two-level hierarchical routing for heterogeneous networks by extending current geographical routing protocol. In the routing process, the expected position of destination in the upper layer with deterministic mobility and the virtual expected zone of destination in the lower layer with random mobility are computed.

In heterogeneous networks, the current works on routing design are mostly based on a hierarchical idea and different strategies for different subnetworks. However for space and air networks, given the limited node resources for computation, storage and bandwidth, multiple strategies will lead to increased network complexity and resource waste. A unified routing strategy to select an end-to-end path in the bundle layer becomes necessary for uniform deployment and centralized management.

IV. UNIFIED NETWORK FRAMEWORK FOR INTEGRATED SPACE/AIR INFORMATION NETWORKS

In this paper, we propose a unified routing framework as shown in Fig. 5, where the strategy of 'divide and conquer' is utilized. The routing mechanism follows a hybrid approach. The overall network is composed of a space network characterized by a deterministic time-space graph and an air network characterized by a semi-deterministic time-space graph. Specifically, we first introduce a discrete time homogeneous semi-Markov model for the air network in order to predict the contact probability and contact time between UAV pairs. Based on the prediction results, a semi-deterministic time-space subgraph is available. While for space networks, since the satellite orbits are fixed, a deterministic time-space subgraph could be obtained directly. Then a hybrid time-space graph for the integrated space/air information network is acquired through combining these two subgraphs. Next, the hybrid time-space graph is transformed into a state-space one, in order to remove time dimension from graph edges. Under the store-carry-forward mechanism in DTN architecture which introduces an overlay above regional lower layer

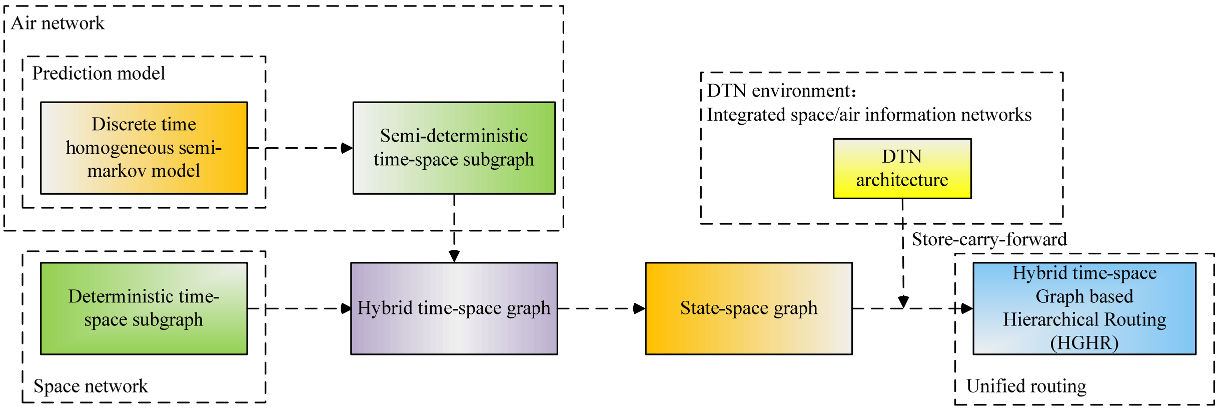

FIGURE 5. Structure diagram of the proposed unified routing framework using 'divide and conquer' strategy, where the routing mechanism follows a hybrid (deterministic/predictable) approach. The overall network is composed of space network characterized by a deterministic time-space graph and air network characterized by a semi-deterministic time-space graph. The DTN architecture introduces an overlay above regional lower layer protocols.

protocols, a data forwarding rule is designed based on the state-space graph. So far, a Hybrid time-space Graph supporting Hierarchical Routing (HGHR) algorithm is finally achieved.

We will introduce the modules of the framework, respectively in the following, by the order of the prediction model, time-space graph the HGHR algorithm. In fact, they are in a progressive relation.

V. PREDICTION MODEL FOR AIR NETWORKS

In this paper, each UAV in the air network maintains its inter-air-mark movement periodically according to a preset flight plan with some random deviations caused by bad weather conditions, fuel shortages and other unexpected cases. This means that all UAVs have their own mobility schedule. Here, each air-mark is regarded as a separate communication unit, i.e., UAVs could only exchange data with others in the same air-mark. Along with the movement rule, UAVs act as data mules for message ferrying incidentally, which can achieve communications among different UAVs, and cooperation with satellites.

In this section, we propose a prediction model to predict the contact time and contact probability for all UAV pairs through analyzing historical information. More specifically, the prediction model is based on a discrete time-homogeneous semi-Markov process, which takes each UAV's historical information including state (air-mark) transition probability and sojourn time probability distribution as inputs. And then the future moving trajectory of each UAV to other air-marks will be predicted so that the contact time and contact probability between all UAV pairs can be obtained.

A. MOTIVATION

Why we need to predict the contact time and contact probability for UAV pairs? We take an example in Fig. 6 to explain it.

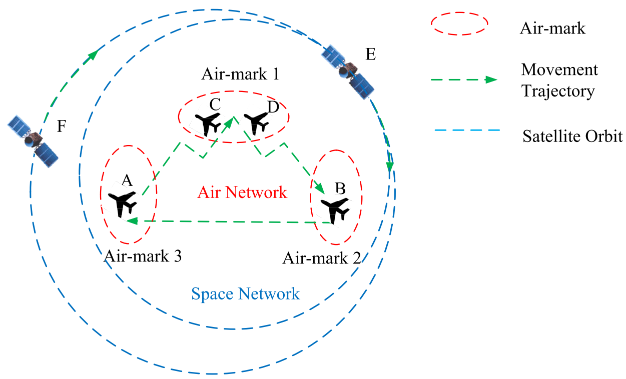

FIGURE 6. Illustration of advantages by predicting the future contact time. Satellites are moving along deterministic orbits and UAVs are inter-air-mark moving.

In the air network, UAVs C and D are both in air-mark 1, while UAVs A and B are in the other two air-marks separately. We imagine that C wants to send data to B. If the system could predict that B will have a contact with D in air-mark 2 earlier than C within an acceptable delay, C will forward the data to D. Then D will leave air-mark 1 and have a contact with B in air-mark 2 for data delivery. Obviously, if we cannot effectively predict the future contact time between C, D and B, it would be possible that C holds the data until encountering B, thus leading to a longer delay of data transmission from C to B. Or in another case, C forwards the data to satellite E, where the long transmission distance may result in unnecessary power consumption for non-emergency data. In summary, the purpose of contact time prediction is to decide whether holding data by the node itself or forwarding data to another.

We will introduce our prediction model next, and the notation list is shown in Table. 1.

B. SEMI-MARKOV MODEL

A semi-Markov model is an extension of Markov model which predicts the future state or state transition direction

TABLE 1. Notation List.

Notations	Meanings
m	A UAV node.
T_{win}	A time window of the integrated information network, and it is equally divided into several time slots.
t	A time slot in T_{win}, and it is an integer.
l	Number of air-marks.
T_{rec}	A recorded time slot, and it is an integer.
S_n^m	The n^{th} state of UAV m, i.e., the air-mark n where the UAV m is currently located at.
T_n^m	The time of the state transition $S_{n-1}^m \rightarrow S_n^m$.
$G_{ij}^m(t)$	The probability that the state transition from the i^{th} state to the j^{th} state of UAV m is completed in the period of time slot 0 to t.
$G_{ij}^m(k)$	The probability that the state transition from the i^{th} state to the j^{th} state of UAV m is completed at time slot k.
P_{ij}^m	The probability of the state transition from the i^{th} state to the j^{th} state of UAV m.
$W_{ij}^m(t)$	The probability that the sojourn time in the i^{th} state of UAV m does not exceed the period of time slot 0 to t, when the next state of UAV m is the j^{th} state.
$tran_i^m$	Number of state transitions from the i^{th} state of UAV m, without considering which state is the next one.
$tran_{ij}^m$	Number of state transitions from the i^{th} state to the j^{th} state of UAV m.
$\xi_{ij}^m(t)$	The probability that the UAV m moves into the air-mark j at the future time slot t on condition that the UAV m is currently located at the i^{th} air-mark.
$G_{ir}^m(h)'$	UAV m has the first transition from the i^{th} state to the r^{th} state at time slot h.
$\rho_{m_a m_b}^j(t)$	The probability that UAVs m_a and m_b will have a contact at the air-mark j in the future time slot t.
$\rho_{m_a m_b}(t)$	The probability that UAVs m_a and m_b will have a contact in the future time slot t, not considering at which air-mark.

according to the current state. In a semi-Markov model, the future state is related not only to the current state but also to the state transition time from the current state to the future state, assuming that the state transition time is instantaneous compared to the long state duration. If the state duration obeys index distribution without Markov property in the semi-Markov process, we can get a time-continuous Markov chain [36] and the state transition time has Markov property.

C. DISCRETE TIME-HOMOGENEOUS SEMI-MARKOV MODEL FOR UAV MOVEMENT

We model the movement of UAV m as a discrete time-homogeneous semi-Markov model (S_n^m, T_n^m), where n refers to the n^{th} state of UAV m, i.e. the air-mark where the UAV m is currently located at. Here, the state transition means that UAV m moves into another air-mark from the current air-mark. Independent of the past state S_{n-1}^m, the state of UAV m is transited from the current state S_n^m to the future state S_{n+1}^m. The variable T_n^m represents the time of the state transition $S_{n-1}^m \rightarrow S_n^m$, so the variable $(T_{n+1}^m - T_n^m)$ represents the sojourn time of UAV m in the n^{th} state, i.e., the duration of maintaining the state S_n^m for UAV m. Since each UAV has its predictable movement trajectory among air-marks, we could predict the movement of UAVs by computing the state transition probability and sojourn time probability distribution.

First of all, based on the discrete time-homogeneous semi-Markov model above, the movement of UAV m can be characterized as follows:

$$\begin{aligned} G_{ij}^m(t) &= P(S_{n+1}^m = j, T_{n+1}^m - T_n^m \le t | S_0^m, \ldots S_n^m; T_0^m, \ldots T_n^m) \\ &= P(S_{n+1}^m = j, T_{n+1}^m - T_n^m \le t | S_n^m = i) \end{aligned} \tag{1}$$

where t is a time slot got from the time window T_{win} of the integrated information network.

Next, we obtain the following equation according to the time discreteness and conditional probability formula:

$$\begin{aligned} G_{ij}^m(t) &= P(S_{n+1}^m = j, T_{n+1}^m - T_n^m \le t | S_n^m = i) \\ &= P(S_{n+1}^m = j | S_n^m = i) \\ &\quad \cdot P(T_{n+1}^m - T_n^m \le t | S_{n+1}^m = j, S_n^m = i) \end{aligned} \tag{2}$$

We define the state transition probability of UAV m as follows:

$$P_{ij}^m = P(S_{n+1}^m = j | S_n^m = i) = \lim_{t \to \infty} G_{ij}^m(t) \tag{3}$$

Assuming the next air-mark is j, we define the sojourn time probability for UAV m currently located at the air-mark i as follows,

$$W_{ij}^m(t) = P(T_{n+1}^m - T_n^m \le t | S_{n+1}^m = j, S_n^m = i) \tag{4}$$

Therefore, Eq. (2) can also be written as follows:

$$G_{ij}^m(t) = P_{ij}^m \cdot W_{ij}^m(t) \tag{5}$$

With the state transition probability P_{ij}^m and sojourn time probability distribution $W_{ij}^m(t)$, we can predict the future movement of UAV m.

1) STATE TRANSITION PROBABILITY

For each UAV, given the total number of states (air-marks) l, we obtain the corresponding state transition probability matrix. For instance, if we totally have 4 air-marks (i.e., l=4), the state transition model of UAV m is shown in Fig. 7(a). Here, P_{ij}^m represents the state transition probability of m from the air-mark i to the air-mark j. For example, P_{12}^m represents the state transition probability of UAV m from the current air-mark 1 to the air-mark 2 in the future. We then determine the state transition probability matrix in Fig. 7(b). We use the following equation to calculate the matrix element P_{ij}^m:

$$P_{ij}^m = tran_{ij}^m / tran_i^m \tag{6}$$

where for UAV m, $tran_i^m$ represents the number of transitions from the air-mark i without considering which air-mark is the next one; $tran_{ij}^m$ is the total numbers of transitions from the air-mark i to the air-mark j. Obviously, we have $tran_{ij}^m \le tran_i^m$ and $P_{ij}^m \le 1$. By keeping track of the historical values of $tran_i^m$ and $tran_{ij}^m$, we generate periodically updated state transition probability matrices of UAV m. For example, within a certain time window, if the total number of transitions from the air-mark 1 is 5 while the total number of transitions from the air-mark 1 to the air-mark 2 is 1, then $P_{12}^m = 1/5$.

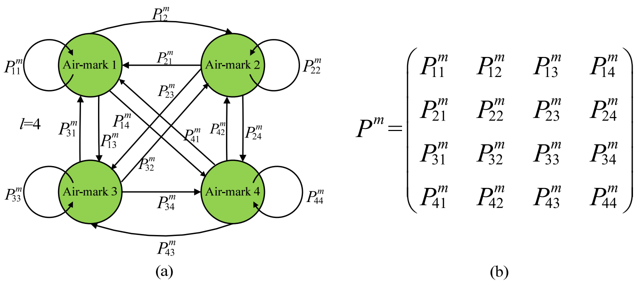

FIGURE 7. Illustration of state transition probability matrix for UAV *m*. Assuming there are 4 air-marks, P_{ij}^m represents the probability that the UAV *m* move to the UAV fomation *j* from *i*. When *i* = *j*, the UAV *m* stay in the original air-mark.

2) SOJOURN TIME PROBABILITY

Before UAV m moves into the air-mark j, we calculate the sojourn time probability of UAV m in the air-mark i using the following equation:

$$W_{ij}^m(t) = P(t_{ij}^m < t) = \sum_{u=0}^{t-1} P(t_{ij}^m = u) \tag{7}$$

where t_{ij}^m is the sojourn time of UAV m in the air-mark i before it moves into the air-mark j. For instance, if we have six historical values of t_{ij}^m within a certain time window, and they are $\{2, 3, 3, 6, 5, 4\}$, we will have $P(t_{ij}^m < 5) = 2/3$.

Similarly, if we know that the state of UAV m is s_{rec} at the time slot T_{rec} ($0<T_{rec}<t$), the sojourn time probability is given in the following equation.

$$W_{s_{rec}j}^m(t - T_{rec}) = \sum_{u=0}^{t-T_{rec}-1} P(t_{s_{rec}j}^m = u) \tag{8}$$

So far, we have finished the prediction for the future movements of UAVs. Based on the aforementioned periodically updated matrices, we will predict the future position of UAVs in the following.

D. PREDICTION FOR UAV POSITION

We let $Y^m = \{Y_t^m, t \in R^+\}$ represent a time-related state set of UAV m. Here, Y_t^m represents the state of UAV m at the time slot t. The transition probability Y_t^m can be described in the following equation.

$$\xi_{ij}^m(t) = P(Y_t^m = j | Y_0^m = i) \tag{9}$$

where, $\xi_{ij}^m(t)$ is the probability that UAV m will move into the air-mark j at the future time slot t on condition that the UAV m is currently located at the air-mark i. Thus, we have two corollaries:

Corollary 1: For UAV m with initial state i. In the future time slot t, we have:

$$\sum_{j=1}^{l} \xi_{ij}^m(t) = 1, \quad \forall m, i, t. \tag{10}$$

Corollary 2: When $t = 0$, UAV m must be in air-mark i, thus we have the following corollary.

$$\xi_{ij}^m(0) = \delta_{ij} = \begin{cases} 1 & i = j \\ 0 & i \neq j \end{cases} \tag{11}$$

When $t > 0$, $\xi_{ij}^m(t)$ provides the prediction for node locations in the future time slot t, if we know the current state of UAV m. We calculate $\xi_{ij}^m(t)$ in two cases:

- Case 1: UAV m is always in air-mark i from time slot 0 to t. Then we have:

$$\begin{aligned} \xi_{ij}^m(t) &= P(Y_t^m = i | Y_0^m = i, T_1^m - T_0^m \geq t) \\ &= P(T_1^m - T_0^m \geq t | Y_0^m = i) \\ &= 1 - W_i^m(t) \end{aligned} \tag{12}$$

  According to Eq. (4), we obtain the following sojourn time probability for UAV m in air-mark i, without considering which air-mark is the next one.

$$W_i^m(t) = P(T_{n+1}^m - T_n^m \leq t | S_n^m = i) = \sum_{j=1}^{l} G_{ij}^m(t) \tag{13}$$

- Case 2: There exists at least one state transition for UAV m from time slot 0 to t. Then we have:

$$\begin{aligned} \xi_{ij}^m(t) &= P(Y_t^m = j | Y_0^m = i, \text{at least one state transition}) \\ &= \sum_{r=1}^{l} \sum_{h=1}^{t-1} G_{ir}^m(h)' \cdot \xi_{rj}^m(t-h) \end{aligned} \tag{14}$$

  where $G_{ir}^m(h)' = G_{ir}^m(h) - G_{ir}^m(h-1)$, which means that UAV m has the first state transition from the i^{th} state to the r^{th} state at the time slot h.

With the consideration of the aforementioned two cases, we determine the following location probability for UAV m:

$$\xi_{ij}^m(t) = [1 - W_i^m(t)] \cdot \delta_{ij} + \sum_{r=1}^{l} \sum_{h=1}^{t-1} G_{ir}^m(h)' \cdot \xi_{rj}^m(t-h) \tag{15}$$

From Eq. (11), we can see that the left term of Eq. (15) becomes 0 when $i \neq j$, which means that UAV m actually has at least one state transition. When $i = j$, it indicates that UAV m'initial state is the i^{th} state, but after that: (i) UAV m may be always in the air-mark i without any state transition, as shown in the left term of Eq. (15); or (ii) UAV m may have at least one state transition as shown in the right term of Eq. (15). Next, Eq. (15) can be converted into the following equation according to the time discreteness:

$$\begin{aligned} \xi_{ij}^m(t) &= P(Y_t^m = j | Y_0^m = i) = c_{ij}^m(t) \\ &\quad + \sum_{r=1}^{l} \sum_{h=1}^{t-1} f_{ir}^m(h) \cdot \xi_{rj}^m(t-h) \end{aligned} \tag{16}$$

where $c_{ij}^m(t) = [1 - W_i^m(t)] \cdot \delta_{ij}$, and

$$f_{ij}^m(t) = \begin{cases} G_{ij}^m(1) & t = 1 \\ G_{ij}^m(t) - G_{ij}^m(t-1) & t > 1 \end{cases}$$

Given the value of $G_{ij}^m(t)$, the value of $\xi_{ij}^m(t)$ depends on $\xi_{ij}^m(t-h)$ computed in previous steps. Thus, the value of $\xi_{ij}^m(t)$ is finally determined using the iteration method.

Similarly, if we know that the state of UAV m is s_{rec} at the time slot T_{rec} ($0<T_{rec}<t$), then after (t-T_{rec}) time slots, at the time slot t, we can get:

$$\xi_{s_{rec}j}^m(t) = P(Y_t^m = j | Y_{T_{rec}}^m = s_{rec}) = c_{s_{rec}j}^m(t - T_{rec}) + \sum_{r=1}^{l} \sum_{h=1}^{t-T_{rec}-1} f_{s_{rec}r}^m(h) \cdot \xi_{rj}^m(t - T_{rec} - h) \quad (17)$$

According to Eq. (16), once the value of $\xi_{ij}^m(t)$ is determined, we then obtain the location probability matrix $M^m(t)$ with the element $\xi_{ij}^m(t)$. As mentioned above, $\xi_{ij}^m(t)$ is the probability that UAV m will move into the air-mark j in the future time slot t on condition that the UAV m is currently located at the air-mark i. For instance, given the total number of air-marks l=4, we will have the following location probability matrix.

$$M^m(t) = \begin{bmatrix} \xi_{11}^m(t) & \xi_{12}^m(t) & \xi_{13}^m(t) & \xi_{14}^m(t) \\ \xi_{21}^m(t) & \xi_{22}^m(t) & \xi_{23}^m(t) & \xi_{24}^m(t) \\ \xi_{31}^m(t) & \xi_{32}^m(t) & \xi_{33}^m(t) & \xi_{34}^m(t) \\ \xi_{41}^m(t) & \xi_{42}^m(t) & \xi_{43}^m(t) & \xi_{44}^m(t) \end{bmatrix}$$

Obviously, the row number (i.e., i) of $M^m(t)$ represents the current air-mark index of UAV m, while the column number (i.e., j) represents the index of the air-mark the UAV m will move into at the future time slot t. Given the index of the current air-mark i, we will find the maximal element value $\xi_{ij^*}^m(t)$ along the i^{th} row of $M^m(t)$, and the corresponding column number j^* is the index of the air-mark the UAV m will move into at the future time slot t. So far, we have determined the future location of UAVs.

E. PREDICTION FOR CONTACT TIME AND CONTACT PROBABILITY

We first define $\xi_{i_aj}^{m_a}(t-t_a)$ as the probability that UAV m_a will arrive at the air-mark j at the future time slot t on condition that the initial state is the air-mark i_a at the time slot t_a. Similarly, $\xi_{i_bj}^{m_b}(t - t_b)$ is the probability that UAV m_b will arrive at the air-mark j at the future time slot t on condition that the initial state is i_b at the time slot t_b. Correspondingly, we determine the probability that UAVs m_a and m_b have a contact in the air-mark j at the future time slot t as follows:

$$\rho_{m_am_b}^j(t) = \xi_{i_aj}^{m_a}(t - t_a) \cdot \xi_{i_bj}^{m_b}(t - t_b), \quad \forall t > 0 \quad (18)$$

Meanwhile, we can also calculate the probability that UAVs m_a and m_b have a contact in any air-mark for each time slot t is as follows:

$$\rho_{m_am_b}(t) = \sum_{j=1}^{l} \rho_{m_am_b}^j(t), \quad \forall t > 0 \quad (19)$$

Note that the calculated probability might be pretty small or even 0 for some time slots, and only when it is larger than a preset threshold, we will take the corresponding time slot as the contact time.

VI. HYBRID TIME-SPACE GRAPH

Since the topology of the integrated space/air information network changes over time and space, in this section, we construct a hybrid time-space graph whose edge weights are contact time and contact probability. The space network could be characterized as a deterministic movement model with the assumption that satellite orbits are pre-determined, while the air network is semi-deterministic due to each UAV's pseudorandom inter-air-mark movement. Therefore, our hybrid time-space graph includes two subgraphs: a deterministic one and a semi-deterministic one whose edge weights need to be predicted by our prediction model.

A. DESCRIPTION OF HYBRID TIME-SPACE GRAPH AND STATE-SPACE GRAPH

We have definitions for the hybrid graph as follows.

Definition 1: we divide the time window T_{win} into a number of small and fixed time slots, and the size of each time slot is symbolized as t_s. Since satellite orbits in the space network are pre-determined, the contact probability between each satellite pair follows the distribution of (0, 1). In other words, we need not predict the contact probability. If a satellite pair has a contact at the time slot t, the corresponding contact can be described by a 2-tuple (t, 1), wherein all the values of t in one satellite movement cycle are known in advance.

Definition 2: For each UAV pair, the discrete contact probability can be represented by a 2-tuple (t, p), where t is a certain time slot, and p represents the contact probability between a UAV pair at the time slot t. The values of t and p can be predicted by our prediction model.

Based on Definition 2, we have the following corollaries:

Corollary 3: Within a list of consecutive time slots, the contact probability may remain constant for a UAV pair. Thus for a certain UAV pair, if they have the same contact probability within successive time slots t_1, t_2, ..., t_n, i.e., p_1=p_2=...=p_n, their contact probability is presented by (t^*, p^*), where t^*=t_1=t_2=...=t_n, and p^*=p_1=p_2=...=p_n.

Corollary 4: For a UAV pair within the time window T_{win}, the number of discrete contacts is equal to or less than T_{win}/t_s which is the number of time slots in T_{win}. Here t_s is the size of each time slot.

Corollary 5: t_s is an important weighing coefficient between prediction accuracy and computational complexity. Greater t_s leads to worse prediction accuracy but lower computational complexity, vice versa.

Definition 3: The UAV with semi-determined movement is not always within the satellite's coverage area. Thus for a pair of UAV and satellite, the contact probability is represented by a 2-tuple (t, p), and the values of t and p can be predicted.

The notations utilized in hybrid time-space graph and transformed state-space graph are listed in Table. 2. In the air network, the semi-deterministic time-space subgraph

TABLE 2. Notation list.

G_h	G	V	Set of UAV nodes.
		E	Set of edges each of which corresponds to a UAV pair and has a list of discrete contact time and contact probability.
		T	Set of time slots.
	$G^{'}$	$V^{'}$	Set of satellite nodes.
		$E^{'}$	Set of edges each of which corresponds to a satellite pair and has a list of discrete contact time and contact probability.
		T	Set of time slots.
G_s		V_s	Set of states each of which contains the node ID and contact time, and represents the contact of the current node with another.
		E_s	Set of time-independent edges each of which has a discrete contact probability and the duration for the state transition.

G=(V, E, T), where V is the set of UAV nodes; E is the set of edges each of which corresponds to a pair of UAVs and has a list of discrete contact time and probability; T is the set of time slots. For the space network, the deterministic time-space subgraph $G^{'}=(V^{'}, E^{'}, T)$, where $V^{'}$ represents the set of satellites, and $E^{'}$ represents the set of edges each of which has a list of discrete contact time and probability between a pair of satellites. Note that our semi-deterministic time-space subgraph also includes the middle part between air and space networks.

For example, given the integrated space/air information network scenario shown in Fig. 6, we can construct a hybrid time-space graph G_h including G and $G^{'}$ shown in Fig. 8 (a), where we consider that a time window T_{win} totally has 60 time slots. We can see that the short dotted edge (E, F) corresponds to the deterministic time-space subgraph for the space network, which is labeled by two contact probabilities (13, 1) and (32, 1), meaning that there are two contacts between satellites E and F at time slot 13 and 32, respectively. Other edges in Fig. 8 (a) comprise a semi-deterministic time-space subgraph for the air network, and each of them contains a set of discrete contact probability. For example, the solid edge (A, B) has two discrete contact probabilities, e.g., $(3, 0.7)$ means that the contact probability is 0.7 for UAVs A and B at the time slot 3.For UAVs, as mentioned above, they must go through the UAV gateway to communicate with satellites. The semi-deterministic time-space subgraph also includes edges between satellites and UAVs. For example, the dotted edge (E, A) is labeled by (3, 0.7), which means that satellite E and UAV gateway A have a contact at the time slot 3 and the corresponding contact probability is 0.7.

Next, we transform the hybrid time-space graph in Fig. 8 (a) into a time-independent state-space graph shown in Fig. 8 (b), in order to eliminate the time dimension of edges. The time-independent state-space graph G_s=(V_s, E_s), where V_s represents a set of states each of which contains the node ID and contact time, while E_s is a set of time-independent edges each of which has a discrete contact probability and the duration for the state transition. Specific description of G_s is as follows:

1) In the hybrid time-space graph, if node u has more than one contact, we create a set of states each of which is denoted as $\{t_i/u\}$ in our state-space graph. For example, in Fig. 8 (a), UAV A has 5 discrete contacts, $(3, 0.7)$, $(7, 0.7)$, $(8, 0.8)$, $(10, 0.5)$ and $(37, 0.7)$, thus we can create the corresponding state set with 5 states $\{3/A\}$, $\{7/A\}$, $\{8/A\}$, $\{10/A\}$ and $\{37/A\}$ in G_s. Note that, if node u contacts with more than one node within the same time slot, we record only one state for u in G_s. For example, UAV A contacts with both satellite E and UAV B at the time slot 3, only one state $\{3/A\}$ is created, thus reducing the graph size.

2) We establish two types of edges in G_s, unidirectional edges and bi-directional edges. As shown in Fig. 8 (b), each node has one state ring, including unidirectional edges connecting all consecutive states, such as UAV A with the state ring including 5 states. Starting from the state with the smallest time slot, the time included in the states keeps increasing along the pointer arrows, and it goes on to the next time window when all states have been traversed. For example, for the state transition from $\{37/A\}$ to $\{3/A\}$, the time slot 3 is in the next time window. In the 2-tuple (t_d, p) of each edge owned by G_s, t_d is not a time slot but the duration for the state transition. Still, taking the edge from $\{37/A\}$ to $\{3/A\}$ as an example, the time in the edge is 26 which means data has stored in node A for 26 time slots. The discrete contact probability contained in each unidirectional edge is always 1 since the initial and final states have the same node ID, which means that data is stored in one node for a period. In another case, a bi-directional edge will be created between states belonging to different nodes, such as states $\{\hat{t}/u\}$ and $\{\hat{t}/v\}$ at the time slot $\hat{t}$ for nodes u and v. Correspondingly, the duration of the state transition is 0, i.e., the data transmission is accomplished during a negligible time; the discrete contact probability between two nodes is always less than 1. For example, the discrete contact probability is 0.7 for the bi-directional edge between $\{3/A\}$ and $\{3/B\}$. For UAVs, they must go through the UAV gateway to communicate with satellites. For example, the bi-directional edge between $\{3/E\}$ and $\{3/B\}$ means a contact between UAV B and satellite E.

B. GENERATION OF HYBRID STATE-SPACE GRAPH AND STATE-SPACE GRAPH

For the air network, we first utilize the periodically updated historical information to generate the transition probability P_{ij}^{m} and sojourn time probability $W_{ij}^{m}(t)$. Then the contact time and contact probability are both predicted according to Eq. (16) using the iteration method. As a result, a semi-deterministic time-space graph is generated. Since the contact time and contact probability are both pre-known in the space network, we obtain a hybrid time-space graph for the integrated information network. To reduce the number of edges in the hybrid graph, the edges with contact probability lower than a threshold are deleted. We transform the simplified hybrid time-space graph into a time-independent state-space graph G_s.

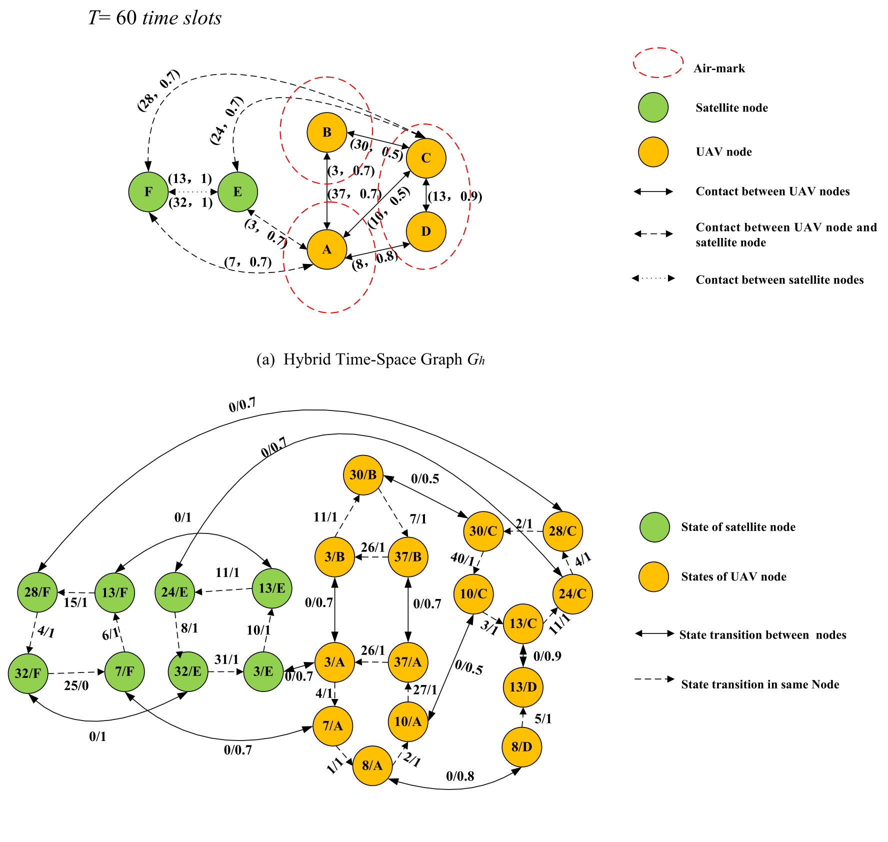

(a) Hybrid Time-Space Graph G_h

(b) State-Space Graph G_s

FIGURE 8. Transformation from time-space graph G_h to state-space graph G_s. We imagine A and C are UAV gateway nodes which could have contacts with satellites. In (a): The nodes represent satellites and UAVs. The edge information is contact time and contact probability. In (b): The nodes are state of satellites and UAVs, which contains contact time and node IDs. The edge information is state duration and contact probability.

The pseudo code of the state-space graph generation algorithm is shown in Algorithm. 1. We describe the steps as follows:

- Step 1: Set the value of the time window T_{win}. Update the state transition probability and sojourn time probability for UAVs within T_{win}.
- Step 2: Obtain the position probability matrix using the iteration method as mentioned in subsection V-D, according to the results of step 1.
- Step 3: Following the position probability matrix, calculate the contact time and contact probability for each UAV pair.
- Step 4: Construct a semi-deterministic time-space subgraph for the air network with the contact information predicted in step 3, and also a deterministic time-space subgraph for the space network according to the pre-known contact information. Delete edges with contact probability lower than the threshold, in order to simplify the hybrid time-space graph.
- Step 5: Transform the simplified hybrid time-space graph into a time-independent state-space graph.

C. TIME COMPLEXITY AND SPACE COMPLEXITY

Obviously, the complexity of the state-space graph generation algorithm mainly depends on the space complexity of the state-space graph G_s and the time complexity of predicting the contact time and contact probability. Among which, the number of the states in G_s depends on the total number of nodes in the network and the number of discrete contacts generated in a time window T_{win}. The number of discrete contacts is proportional to the number of time slots within T_{win}, and it is inversely proportional to the size of each time slot t_s. Thus, the space complexity of G_s is $\Theta\lceil N \cdot (T/t_s)\rceil$. Here, $N = |V|+|V^{'}|$. Besides, we obtain the time complexity of predicting the contact time and contact probability as $\Theta\lceil N^{'} \cdot l^2 \cdot (T/t_s)^2\rceil$. Here, $N^{'} = |V|$.

VII. UNIFIED ROUTING FOR THE INTEGRATED SPACE/AIR INFORMATION NETWORK

Based on the hybrid time-space graph, we design a data-forwarding rule that is Hybrid time-space Graph supporting Hierarchical Routing (HGHR) algorithm in this section. In general, HGHR transfers data along the path which reduces power resumption and also end-to-end delay. Different from

Algorithm 1 State-Space Graph Generation Algorithm

Input: Time window T_{win}, the size of each time slot t_s, number of air-marks in the network l and probability threshold value Th

Output: state graph G_s;

for all time slots $t = 0$ **to** T/t_s **do**
  for m=1,2,...,$|V|$ **do**
    for initial state $i = 1$ **to** l **do**
      for next state $j = 1$ **to** l **do**
        $P_{ij}^m = tran_{ij}^m / tran_i^m$
        for all $u = 0$ to T/t_s **do**
          $W_{ij}^m(t) = W_{ij}^m(t) + P(t_{ij}^m = u)$
        end for
        $G_{ij}^m(t) = P_{ij}^m \cdot W_{ij}^m(t)$
        if $i = j$ **then**
          $\xi_{ij}^m(0) = 1$
          for relay state $r = 1$ to l **do**
            for relay state $h = 1$ to $t - 1$ **do**
              $\xi_{ij}^m(t) = \xi_{ij}^m(t) + G_{ij}^m(h)' \cdot \xi_{rj}^m(t-h)$
            end for
          end for
          $\xi_{ij}^m(t) = \xi_{ij}^m(t) + [1 - W_i^m(t)]$
        else
          $\xi_{ij}^m(0) = 0$
          for $r = 1$ to l **do**
            for $h = 1$ to $t - 1$ **do**
              $\xi_{ij}^m(t) = \xi_{ij}^m(t) + G_{ij}^m(h)' \cdot \xi_{rj}^m(t-h)$
            end for
          end for
        end if
      end for
    end for
  end for
end for
for all pairs of nodes **do**
  for $j = 1$ **to** l **do**
    $\rho_{m_a m_b}(t) = \xi_{iaj}^{m_a}(t) \cdot \xi_{ibj}^{m_b}(t), \forall t > 0$
    $\rho_{m_a m_b}(t) = \rho_{m_a m_b}(t) + \rho_{m_a m_b}^j(t)$
  end for
end for
Initialize G_h
if $\rho_{m_a m_b}(t) > Th$ **then**
  add new edge containing $\rho_{m_a m_b}(t)$ and t **to** G_h
end if
Return state-graph G_s

static networks, each time the data is forwarded to its neighboring node in proper time, the state-space graph is updated and a new path is selected. Data is transferred hop by hop in the direction of closing to the destination.

We assume the power assumption of per unit data amount is ω_{ij}, then the total power assumption of transmitting data with the amount of x_{ij} in a link e_{ij} is $x_{ij} \cdot \omega_{ij}$. We assume d_m and d_0 as delivery time and request time respectively for a message. For a *path* in the feasible path set *FPath*, we define an objective function as follows, where α and β are two weighting factors for adjusting the proportion of the two metrics: power consumption and delay. And there are three constraints: flow conservation where f_{sd} is a flow demand in a path, link capacity c_{ij} and the time-to-live of messages that is the delay threshold T.

Algorithm 2 Hybrid State-Space Graph Supporting Hierarchical Routing Algorithm

Input: state-graph G_s, link capacity c_{ij}, link power assumption ω_{ij}, source node S, destination node D, request time d_0, delay threshold T.

Output: delivery time d_m, minimum function *minf*

d_m=0,*minf*=0
while $rel \neq D$ **do**
  GF=UpdateGraph(G_s,c_{ij})
  for all $path \in$ feasible path set *FPath* **do**
    $minf = \infty$
    $f = (\sum_{e_{ij} \in path} x_{ij} \cdot \omega_{ij})^\alpha \cdot (d_m - d_0)^\beta$
    if $f < minf$ **then**
      $minf = f$
      $path^* = path$
    end if
  end for
  $rel \leftarrow$ next hop in $path^*$
  $d_m \leftarrow$ delivery time in $path^*$
end while
Return rel, d_m, $minf$

$$\min_{path \in FPath} \left(\sum_{e_{ij} \in path} x_{ij} \cdot \omega_{ij}\right)^\alpha \cdot (d_m - d_0)^\beta$$
$$\text{s.t.} \sum_{e_{ij} \in path} x_{ij} - \sum_{e_{ji} \in path} x_{ji} = \begin{cases} f_{sd} & i = S \\ -f_{sd} & j = D \\ 0 & otherwise \end{cases}$$
$$0 \le x_{ij} \le c_{ij}$$
$$d_m - d_0 \le T \tag{20}$$

The power consumption per unit amount data for each link is obtained in advance. We add an initial state into G_s based on the current time slot and the source node carrying data. Then we can compute the value of the objective function for all feasible paths between the initial and final states, and the path with the minimum value defined as *minf* will be selected. The data is delivered to the next state along the path. It should be noted that the selected next state in the state-space graph may belong to the original node, i.e., data need to be stored in the original node for a period. When the data arrive at the next state along the path, G_s will be updated to obtain a new valid path. Note that G_s is updated every time slot during the initial phase until it has become basically stable. The pseudo code of the HGHR algorithm is shown in Algorithm. 2.

As an example in Fig. 9. Imagine UAV A initiate a routing request to UAV C at the 4^{th} time slot, then $4/A$ is added

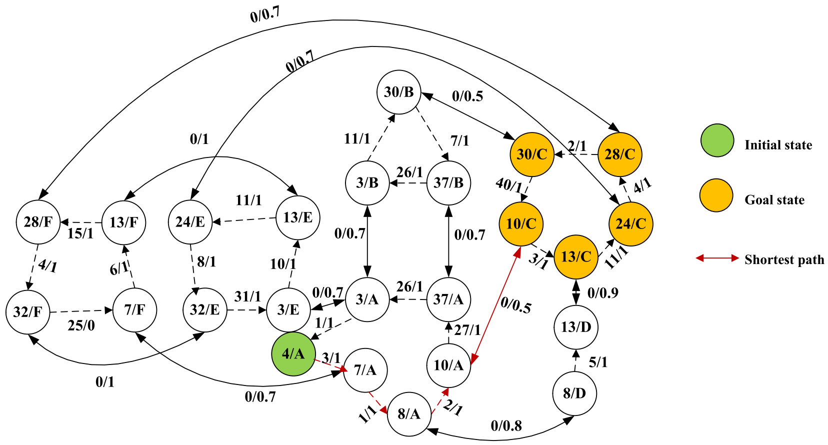

FIGURE 9. Illustration of a shortest path from UAV *A* to UAV *C*. Imagine UAV *A* needs to forward data to UAV *C*. A shortest path is found according to the forwarding rule and the delivery time is 10.

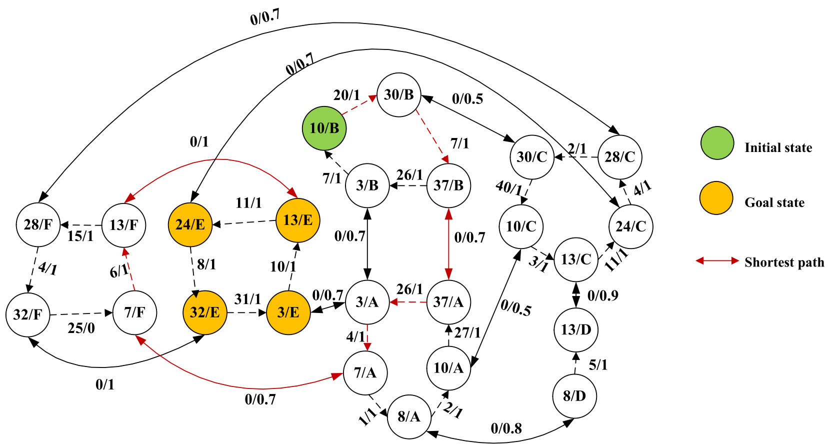

FIGURE 10. Illustration of a shortest path from UAV *A* to satellite *C*. Imagine UAV *A* needs to forward data to satellite *E*. A shortest path is found according to the forwarding rule and the delivery time is 13.

to G_s since it is the 4^{th} time slot currently and the source node is UAV A. Then, all states of the destination node are marked as final states, and we seek to find the best path with $minf$ from $4/A$ to any final state. Another example in Fig. 10 shows the shortest path from UAV B and satellite E. It is a remarkable fact that it must go through the gateway of UAV A to communicate with satellite F.

VIII. PERFORMANCE EVALUATION

In this section, we evaluate the effectiveness of our prediction model and the HGHR algorithm. Specifically, the accuracy of the semi-Markov prediction algorithm is tested. To choose a suitable size of the time slot, we balance the algorithm complexity and also prediction accuracy. Given the contact information between satellites and also between satellites and UAV gateways, we compare our HGHR algorithm with Contact Graph Routing (CGR) [20], Direct strategy and Epidemic routing [29] in terms of end-to-end delay, delivery ratio and power cost.

A. CONTACT INFORMATION SOURCE

To evaluate the effectiveness of our HGHR algorithm, we need to find a way to get the reasonable contact information between satellites and also between UAVs.

TABLE 3. Parameter setting of the network architecture.

parameter name	settings
satellite constellation	Walker 6/6/1, RAAN 240
seeding satellite orbit	circular, 1414km, inclination 52, RAAN 0
ground station	Miyun (40N, 117E)
air-mark range	26S∼29S, 38W∼42.5W

1) CONTACT BETWEEN SATELLITES AND UAV GATEWAYS

The contact information between satellites is deterministic as mentioned above. To obtain reasonable contact information between satellites and UAV gateways, we built a network model assisted by Satellite Tool Kit (STK) software, with experimental ephemeris data for 24 hours from 4^{th}, July, 2015. The parameter settings are listed in Table 3. The $2D$ and $3D$ network models are shown in Fig. 11.

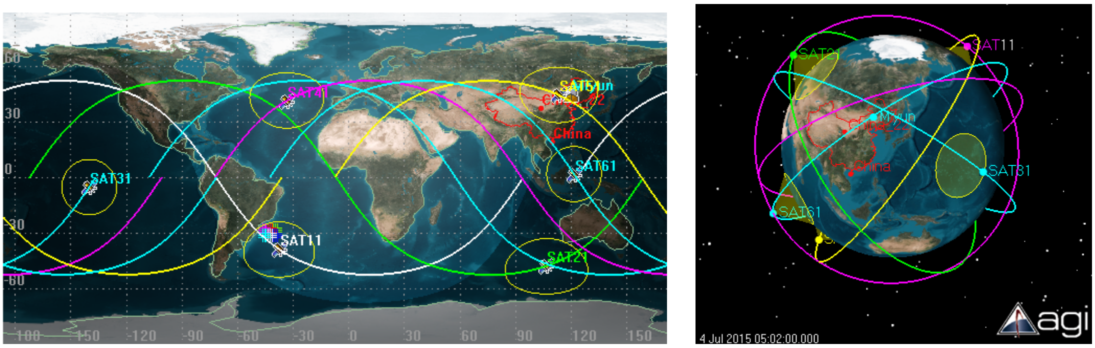

(a) 2D network model (c) 3D network model

FIGURE 11. Network architectures in 2D/3D modes in STK. (a) 2D network model (c) 3D network model.

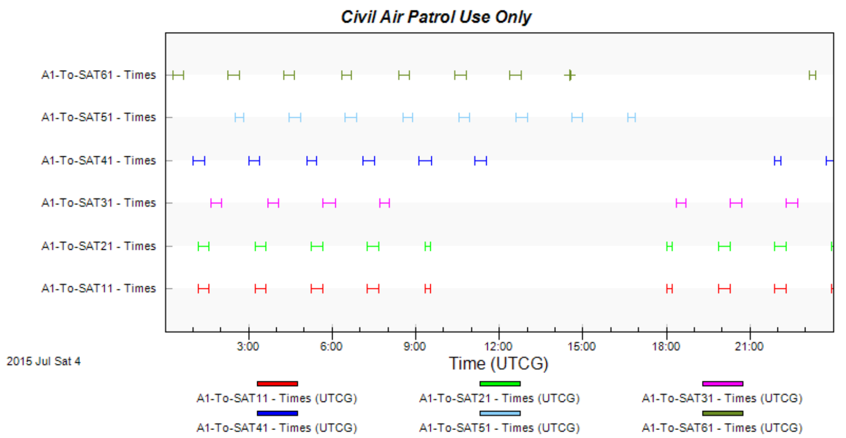

FIGURE 12. Illustration of access between UAV gateway A_1 and satellites.

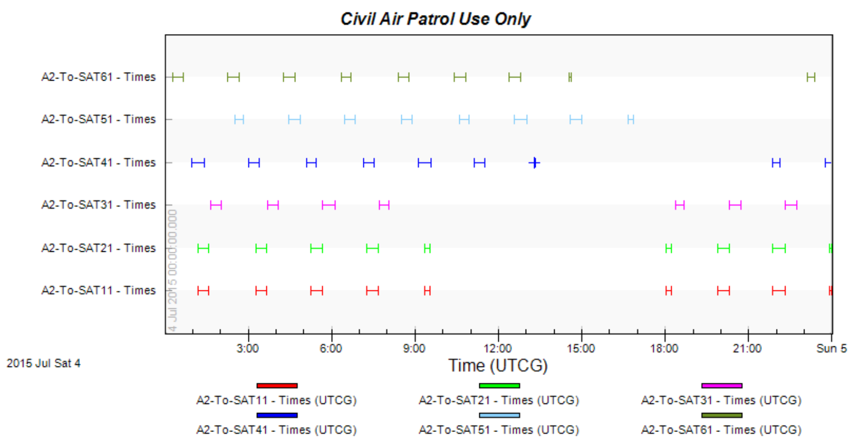

FIGURE 13. Illustration of access between UAV gateway A_2 and satellites.

We analyze the visibility of the satellite constellation to the UAV gateways A_1, A_2 and get the following visible periods as shown in Fig. 12, 13, most of which are at least 12 minutes. The figures show that the space network is not always accessible to air networks. We take the data as contact time between satellites and UAV gateways.

2) CONTACT BETWEEN UAVs

In our simulations, each UAV moves among different air-marks and the air network model is shown in Fig. 14. Here, we introduce a moving probability value p_d for UAVs in the air network, which means that each UAV has a probability of moving into a certain air-mark p_d, and also has a probability

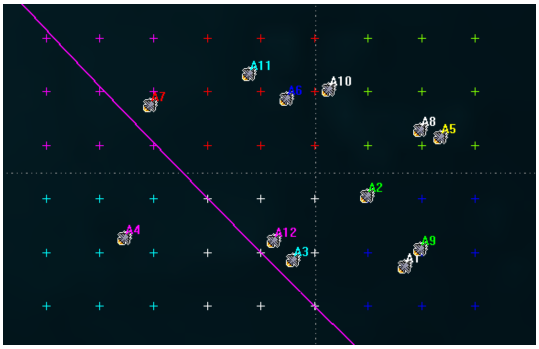

FIGURE 14. Air network model in STK.

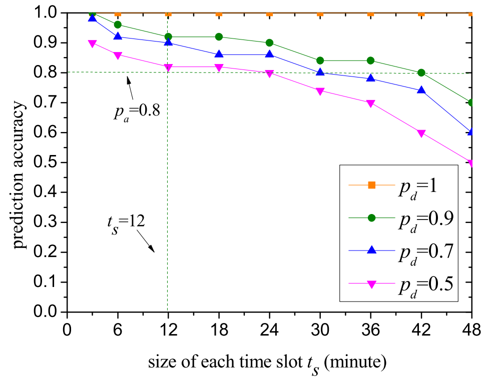

FIGURE 15. Variation of prediction accuracy p_a.

TABLE 4. Parameter setting of the network model.

parameter name	default	range
weighting factors (α, β)	0.5	╲
number of satellites	6	╲
number of air-marks l	6	4∼8
number of UAVs	12	6∼18
number of UAV gateways	2	╲
UAV speed	200 km/h	100∼240
deterministic rate (p_d)	╲	0.5∼0.9
time window (T_{win})	1 day	╲
message time-to-live (T)	2 hours	1∼3 hours
time slot t_s	╲	6∼48 minutes
contact probability threshold (Th)	0.7	╲

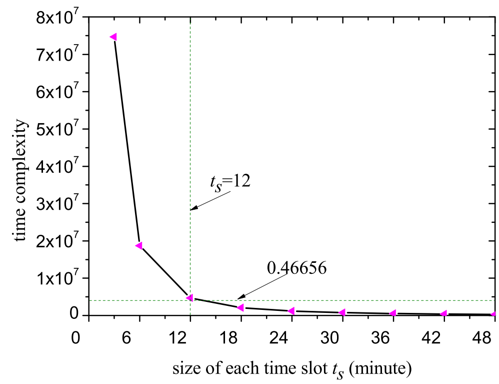

FIGURE 16. Variation of time complexity.

of moving into any other air-marks $(1 - p_d)/(l - 1)$. The probability value p_d represents the deterministic degree of the UAV trajectory. More specifically, The greater p_d is, the more deterministic the UAV trajectory is. The value of p_d is less than 1 to ensure the semi-deterministic characteristic of the air network. According to [37], a UAV has a speed of 30∼460 km/h. The value of p_d, UAV speed and also other parameter settings are listed in Table 4. If without specification, the parameters take default values below.

B. PERFORMANCE COMPARISON

At first, our HGHR program runs for multiple iterations to collect enough historical information until it converges to a stable state. It is a gradual process that the prediction accuracy, i.e., the accuracy of predicting contact time and contact probability becomes increasingly high.

1) PREDICTION ACCURACY p_a

The size of each time slot, i.e., t_s is an important weighing coefficient between prediction accuracy and computational complexity. We test the prediction accuracy in the network with 6 air-marks under various values of t_s and obtain several average value curves of different p_d from 100 prediction results in Fig. 15.

We can see that with the decrease of p_d, the randomness of UAVs' movement increases, thus leading to a slight decline in the prediction accuracy. In the extreme case of p_d=1, the air network becomes deterministic with 100% prediction accuracy. We can also find that as t_s increases, the prediction accuracy decreases. That is because the system cannot record enough transition information including the transition probability and sojourn time probability if t_s becomes too large. Additionally, we have acquired the time complexity of HGHR algorithm in section VI-C. Fig. 16 shows the variation trend of the time complexity with the increasing size of t_s. To get the trade-off between the time complexity and prediction accuracy, we let t_s=12 minutes in the following simulations in terms of packet delivery ratio, end-to-end delay and power cost. Thus, we totally have 120 time slots within each time window.

2) END-TO-END DELAY

Compared with the data waiting time in a node of the path, the data delivering time is within 1 time slot (usually tens of milliseconds), which can be ignorable. Thus in our simulations, the end-to-end delay is calculated as the total waiting time in the nodes of the path. Note that it does not include the delays of failed messages which are expired within the time-to-live. We take 2 UAVs as a source-destination pair. Since communication channels are constructed by node movements in this DTN network, the end-to-end delay is relatively long.

With a varying number of air-marks, the comparative results of the end-to-end delay among various routing algorithms are shown in Fig. 17. The Epidemic routing

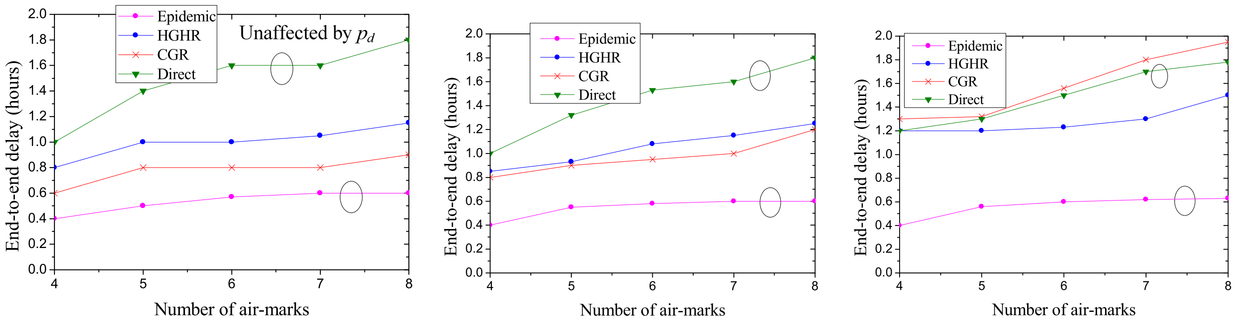

(a) p_d=0.9 (b) p_d=0.7 (c) p_d=0.5

FIGURE 17. Comparisons of end-to-end delay with a varying number of air-marks. (a) $p_d = 0.9$. (b) $p_d = 0.7$. (c) $p_d = 0.5$.

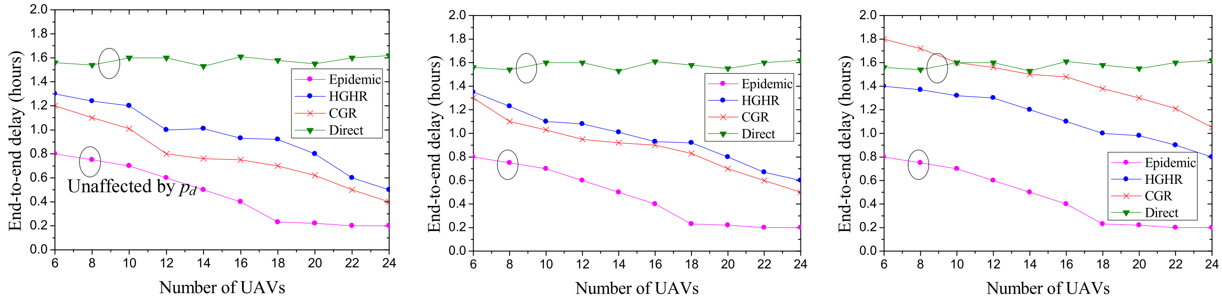

(a) p_d=0.9 (b) p_d=0.7 (c) p_d=0.5

FIGURE 18. Comparisons of end-to-end delay with a varying number of UAVs. (a) $p_d = 0.9$. (b) $p_d = 0.7$. (c) $p_d = 0.5$.

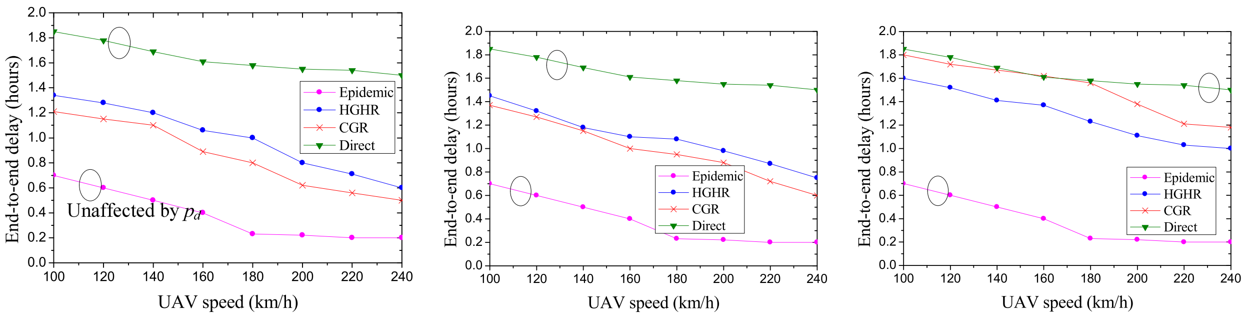

(a) p_d=0.9 (b) p_d=0.7 (c) p_d=0.5

FIGURE 19. Comparisons of end-to-end delay with a varying UAV speed. (a) $p_d = 0.9$. (b) $p_d = 0.7$. (c) $p_d = 0.5$.

performs best and the Direct routing has the poorest performance, both of which are independent of the air network's deterministic degree since no prior knowledge is used. The reason is obvious that the former is multi-path routing by creating copies and there is no forwarding occurs in the latter routing process. CGR performs well especially in the case of p_d=0.9, i.e., the network is nearly deterministic. However, as p_d decreases, it has worse performance than HGHR. That is because CGR utilizes the prior knowledge of networks, without predicting and updating process, in order to find a path with minimal delay. However, in the semi-deterministic network, the topology is changing over time and the calculated path may be no longer valid. Our HGHR has a satisfactory performance because it only selects the next hop which is closer to the destination. Besides, the prediction model works for collecting and updating the semi-deterministic contact information in advance. However, the end-to-end delay becomes larger as the number of air-marks increases. That's because the contact probability between two UAVs decreases.

Fig. 18 shows the comparisons of end-to-end delay with a varying number of UAVs among the above four routing algorithms. For the same reason as stated above, the Epidemic performs best, Direct performs worst, and CGR performs worse as p_d decreases. Except for Direct, the end-to-end delay of the three routing becomes shorter as the number of UAVs increases since there are more relay nodes can be selected to obtain a shorter delay.

Besides, under various UAV speed conditions, Fig. 19 shows the comparative results of the end-to-end delay among

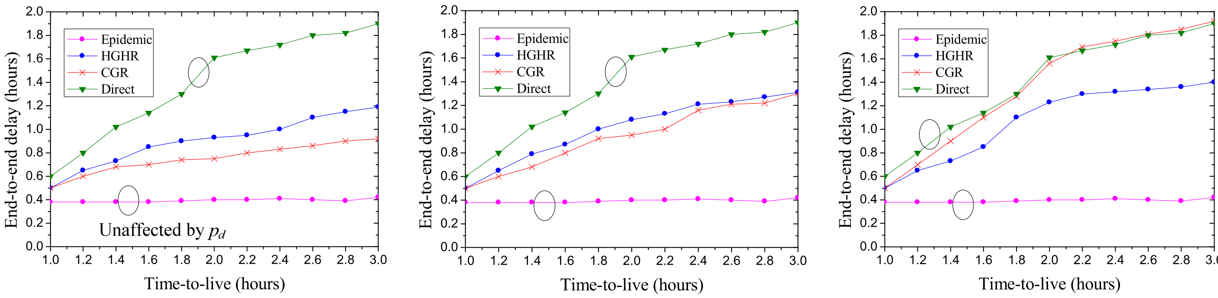

(a) p_d=0.9 (b) p_d=0.7 (c) p_d=0.5

FIGURE 20. **Comparisons of end-to-end delay with a varying time-to-live value. (a) $p_d = 0.9$. (b) $p_d = 0.7$. (c) $p_d = 0.5$.**

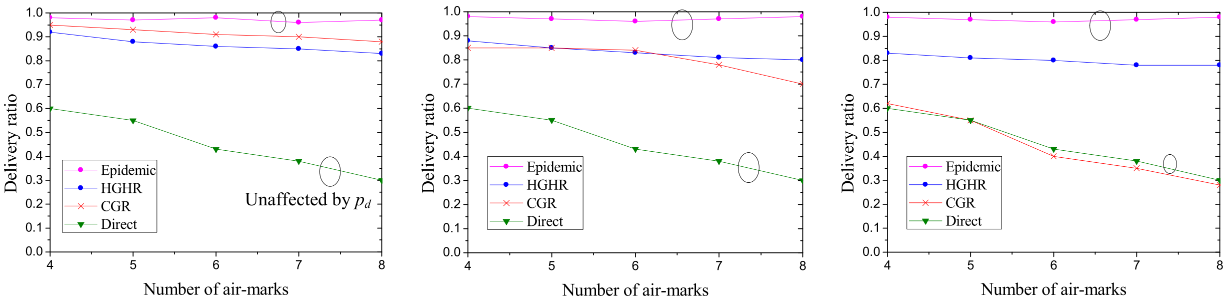

(a) p_d=0.9 (b) p_d=0.7 (c) p_d=0.5

FIGURE 21. **Comparisons of delivery ratio with a varying number of air-marks. (a) $p_d = 0.9$. (b) $p_d = 0.7$. (c) $p_d = 0.5$.**

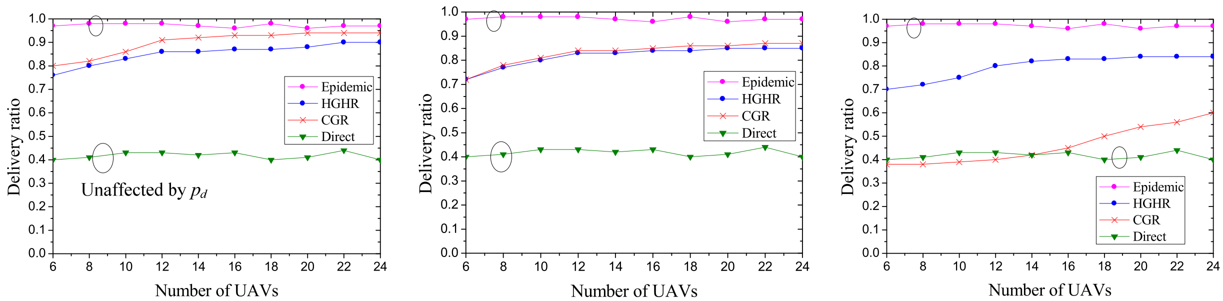

(a) p_d=0.9 (b) p_d=0.7 (c) p_d=0.5

FIGURE 22. **Comparisons of delivery ratio with a varying number of UAVs. (a) $p_d = 0.9$. (b) $p_d = 0.7$. (c) $p_d = 0.5$.**

different routing algorithms. We can see that faster UAV speed brings shorter end-to-end delay in the routing processes, where UAVs are taken as ferries. The comparative results of end-to-end delay with a varying time-to-live value are shown in Fig. 20. The end-to-end delay of HGHR, CGR and Direct becomes larger as the time-to-live value increases. That's because the delay only includes the time for delivered messages. When the time-to-live becomes larger, those messages with long delays are no longer be expired.

3) DELIVERY RATIO

It is the ratio of the number of successfully delivered messages over the total number of messages in the network. It is relative to delays since long delays will result in more expired messages.

We also take 2 UAVs as a source-destination pair and the comparisons of delivery ratio with a varying number of air-marks are shown in Fig. 21. We can see that Epidemic routing could almost achieve a delivery ratio of 100% thanks to the multiple copies. The Direct routing has a low delivery ratio due to its long delays. CGR performs bad when p_d is small. As the number of air-marks increases, the delivery ratio of the HGHR, CGR, Direct decreases.

Fig. 22 shows the comparative results of delivery ratio with a varying number of UAVs. We can get that the Epidemic and Direct have nothing to do with the number of UAVs and also the air network's deterministic degree. But the delivery ratio of the CGR and HGHR has a slight increase with the increasing number of UAVs, i.e. relays. CGR is only suitable for deterministic networks and it will have a high message drop rate when p_d is small.

Besides, the comparisons of delivery ratio with varying UAV speed and also time-to-live value are given in Fig. 23 and Fig. 24, which also show that the Epidemic

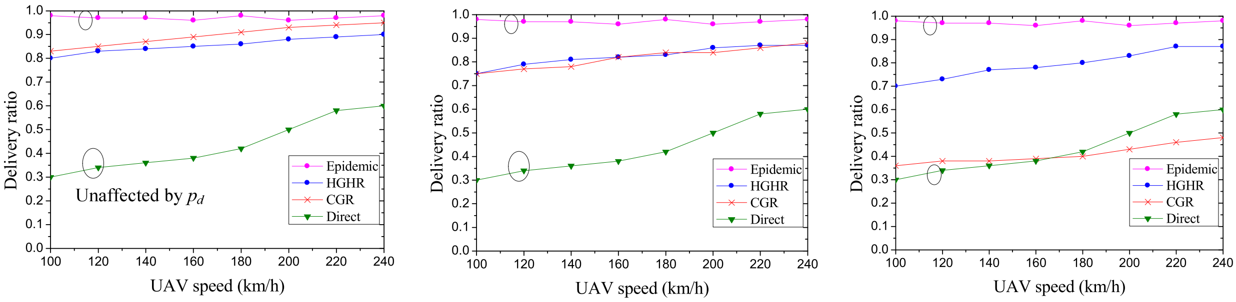

(a) p_d=0.9 (b) p_d=0.7 (c) p_d=0.5

FIGURE 23. Comparisons of delivery ratio with varying UAV speed. (a) $p_d = 0.9$. (b) $p_d = 0.7$. (c) $p_d = 0.5$.

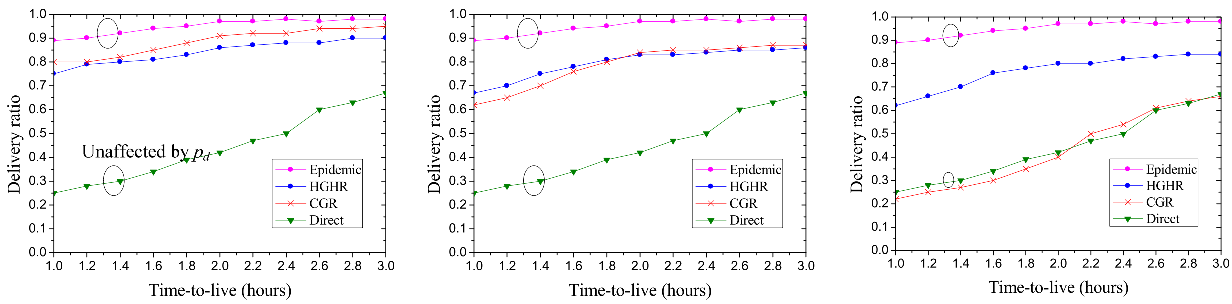

(a) p_d=0.9 (b) p_d=0.7 (c) p_d=0.5

FIGURE 24. Comparisons of delivery ratio with a varying time-to-live value. (a) $p_d = 0.9$. (b) $p_d = 0.7$. (c) $p_d = 0.5$.

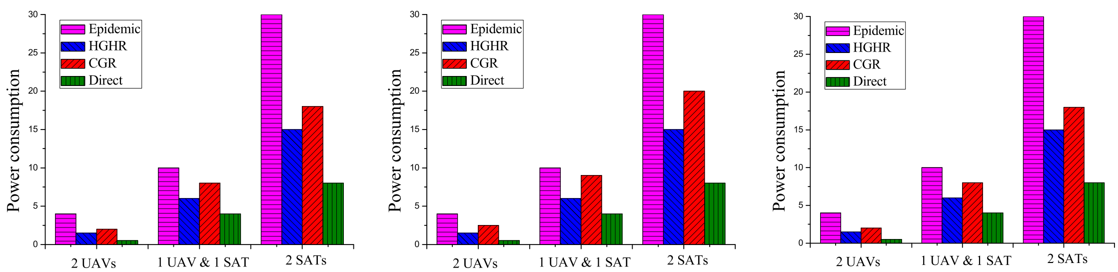

(a) p_d=0.9 (b) p_d=0.7 (c) p_d=0.5

FIGURE 25. Comparisons of power consumption with different kind of source-destination pair. (a) $p_d = 0.9$. (b) $p_d = 0.7$. (c) $p_d = 0.5$.

could achieve a high and reliable delivery ratio while the Direct has a very low delivery ratio. Our HGHR has acceptable delivery ratio while CGR only works well when the network is relatively deterministic. The increase of both UAV speed and time-to-live contributes to improving the delivery ratio. Here, we have to say that we imagine contacts can always happen when two UAVs are in the same air-mark, irrelevant to the UAV speed.

4) POWER CONSUMPTION

We compare the power consumption of different routing algorithms, with different kind of source-destination pair: 2 UAVs, 1 UAV &1 satellite and 2 satellites. We set the different quantitative value of power consumption per unit amount data for satellite links and UAV links. Fig. 25 shows the proportional comparison results. We can easily see that the Epidemic routing has the largest power consumption because it has many copies to transmit. The Direct routing is most energy-efficient since it has no relay forwarding. CGR has more power consumption even in the relatively deterministic network. The reason is that CGR just considers the delay as the path metric while HGHR takes both delay and power consumption as metrics. Note that, although transferring data through satellites could gain a short delay, it brings high power consumption.

IX. CONCLUSION AND FUTURE WORK

In this paper, a unified routing framework by the 'divide and conquer' strategy has been designed for the integrated space/air information network. Specifically, we have built a discrete time-homogeneous semi-Markov model to predict the contact time and contact probability between UAVs in the air network. On the basis of this, a semi-deterministic time-space subgraph has been constructed. Through integrating the deterministic time-space subgraph for the space network with the semi-deterministic time-space subgraph, we have obtained a hybrid time-space graph, and then transformed this graph model into a state-space graph for easy route query. Finally, an HGHR algorithm has been formed, by adopting a message forwarding rule in the state-space graph under the store-carry-forward mechanism. Simulation results have demonstrated that our prediction model has a high prediction accuracy, and our proposed HGHR algorithm effectively improves the delivery ratio, decreases the end-to-end delay and also power consumption.

Some future work remains to be done, mainly including the following possible directions: (i) *a new prediction model for the air network.* Our proposed prediction model can only predict which air-mark a UAV will move into in the future, though it is enough to get contact information in this paper. Other prediction models such as data mining can be utilized to obtain the detailed edge information, so that the routing performances may be further improved. (ii) *routing algorithms for the integrated space-air-ground network including other types of nodes in air or terrestrial networks.* In this paper, the ground end users are not taken into consideration, which is an important part in future integrated networks. We expect to do more work on dynamic routing to adapt to the traffic changes and achieve the network load balance.

REFERENCES

[1] L. Gupta, R. Jain, and G. Vaszkun, "Survey of important issues in UAV communication networks," *IEEE Commun. Surv. Tuts.*, vol. 18, no. 2, pp. 1123–1152, May 2015.

[2] I. Bekmezci, O. K. Sahingoz, and Ş. Temel, "Flying ad-hoc networks (FANETs): A survey," *Ad Hoc Netw.*, vol. 11, no. 3, pp. 1254–1270, 2013.

[3] A. McMahon and S. Farrell, "Delay- and disruption-tolerant networking," *IEEE Int. Comput.*, vol. 13, no. 6, pp. 82–87, Nov. 2009.

[4] K. Fall, "A delay-tolerant network architecture for challenged internets," in *Proc. Conf. Appli., Technol., Archit. Protocols Comput. Commun.*, Aug. 2003, pp. 27–34.

[5] V. V. Gounder, R. Prakash, and H. Abu-Amara, "Routing in LEO-based satellite networks," in *Proc. Emerging Technol. Symp. Wireless Commun. Syst.*, Apr. 1999, pp. 22.1–22.6.

[6] B. Gu and X. Hong, "Capacity-aware routing using throw-boxes," in *Proc. IEEE Int. Global Telecommum. Conf. (GLOBECOM)*, Dec. 2011, pp. 1–5.

[7] A. Casteigts, P. Flocchini, W. Quattrociocchi, and N. Santoro, "Time-varying graphs and dynamic networks," *Int. J. Parallel, Emergent Distrib. Syst.*, vol. 27, no. 5, pp. 387–408, Apr. 2012.

[8] M. Huang, S. Chen, Y. Zhu, and Y. Wang, "Topology control for time-evolving and predictable delay-tolerant networks," *IEEE Trans. Comput.*, vol. 62, no. 11, pp. 2308–2321, Nov. 2013.

[9] Y. Quan, I. Cardei, and J. Wu, "An efficient prediction-based routing in disruption-tolerant networks," *IEEE Trans. Parallel Distrib. Syst.*, vol. 23, no. 1, pp. 19–31, Jan. 2012.

[10] P. Liu, K. Jia, and Y. Zhang, "A layered structure prediction method for mode decision in video encoding," in *Proc. 8th Int. Conf. Intell. Inf. Hiding Multimedia Signal Process. (IIH-MSP)*, Jul. 2012, pp. 407–410.

[11] Y. Li, J. Zhang, J. Xiao, and Y. Tan, "Short-term prediction of the output power of PV system based on improved grey prediction model," in *Proc. Int. Conf. Adv. Mech. Syst.*, Aug. 2014, pp. 547–551.

[12] V. B. Nikam and B. B. Meshram, "Modeling rainfall prediction using data mining method: A Bayesian approach," in *Proc. 4th Int. Conf. Comput. Intell., Model. Simul. (CIMSim)*, Sep. 2013, pp. 132–136.

[13] Y. Cao and Z. Sun, "Routing in delay/disruption tolerant networks: A taxonomy, survey and challenges," *IEEE Commun. Surv. Tuts.*, vol. 15, no. 2, pp. 654–677, 2nd Quart. 2013.

[14] M. J. Khabbaz, C. M. Assi, and W. F. Fawaz, "Disruption-tolerant networking: A comprehensive survey on recent developments and persisting challenges," *IEEE Commun. Surv. Tuts.*, vol. 14, no. 2, pp. 607–640, 2nd Quart. 2012.

[15] S. Jain, K. Fall, and R. Patra, "Routing in a delay tolerant network," *Computer. Commun. Review.*, vol. 34., no. 4, pp. 145–158, Oct. 2004.

[16] D. Fischer, D. Basin, and T. Engel, "Topology dynamics and routing for predictable mobile networks," in *Proc. IEEE Int. Conf. Netw. Protocols (ICNP)*, Oct. 2008, pp. 207–217.

[17] S. Merugu, M. Ammar, and A. E. Zegura, "Routing in space and time in networks with predictable mobility," Georgia Inst. Technol. College Eng., Atlanta, GA, USA, Tech. Rep. GIT-CC-04-7, 2004. [Online]. Available: https://smartech.gatech.edu/bitstream/handle/1853/6492/GIT-CC-04-07.pdf

[18] C. Caini, H. Cruickshank, S. Farrell, and M. Marchese, "Delay- and disruption-tolerant networking (DTN): An alternative solution for future satellite networking applications," *Proc. IEEE*, vol. 99, no. 11, pp. 1980–1997, Nov. 2011.

[19] S. Burleigh. (2010). *Contact Graph Routing and it is an IETF Internet-1095 Draft*. [Online]. Available: https://tools.ietf.org/html/draft-burleigh-dtnrg-cgr-00

[20] G. Araniti *et al.*, "Contact graph routing in DTN space networks: Overview, enhancements and performance," *IEEE Commun. Mag.*, vol. 53, no. 3, pp. 38–46, Mar. 2015.

[21] J. Segui, E. Jennings, and S. Burleigh, "Enhancing contact graph routing for delay tolerant space networking," in *Proc. IEEE Global Telecommum. Conf. (GLOBECOM)*, Dec. 2011, pp. 1–6.

[22] J. Leguay, T. Friedman, and V. Conan, "DTN routing in a mobility pattern space," in *Proc. ACM SIGCOMM Workshop Delay-Tolerant Netw.*, Apr. 2005, pp. 276–283.

[23] P. Costa, C. Mascolo, M. Musolesi, and G. P. Picco, "Socially-aware routing for publish-subscribe in delay-tolerant mobile ad hoc networks," *IEEE J. Sel. Areas Commun.*, vol. 26, no. 5, pp. 748–760, Jun. 2008.

[24] X. F. Guo and M. C. Chan, "Plankton: An efficient DTN routing algorithm," in *Proc. 10th Annu. IEEE Commun. Soc. Conf. Sensor, Mesh Ad Hoc Commun. Netw. (SECON)*, Jun. 2013, pp. 550–558.

[25] F. Dang, X. Yang, and K. Long, "Spray forwarding algorithm: A dtn routing algorithm based on the Markov position prediction," *Channel Sci., Info. Sci.*, vol. 40, no. 10, pp. 1312–1320, Aug. 2010.

[26] M. Musolesi, S. Hailes, and C. Mascolo, "Adaptive routing for intermittently connected mobile ad hoc networks," in *Proc. 6th IEEE Int. Symp. World Wireless Mobile Multimedia Netw.*, Jun. 2005, pp. 183–189.

[27] D. Rothfus, C. Dunning, and X. Chen, "Social-similarity-based routing algorithm in delay tolerant networks," in *Proc. IEEE Int. Conf. Commun. (ICC)*, Jun. 2013, pp. 1862–1866.

[28] T. D. Tlsty and P. W. Hein, "Know thy neighbor: stromal cells can contribute oncogenic signals," *Current Opinion Genet. Develop.*, vol. 11, no. 1, pp. 54–59, Feb. 2001.

[29] A. Vahdat and D. Becker, "Epidemic routing for partially connected ad hoc networks," Dept. Comput. Sci., Duke Univ., Durham, NC, USA, Tech. Rep. CS-200006, 2000. [Online]. Available: ftp://sweb.cs.duke.edu/dist/techreport/2000/2000-06.ps

[30] R. Diana, E. Lochin, L. Franck, C. Baudoin, E. Dubois, and P. Gelard, "A DTN routing scheme for quasi-deterministic networks with application to LEO satellites topology," in *Proc. IEEE Veh. Technol. Conf. (VTC Fall)*, Sep. 2012, pp. 1–5.

[31] V. Erramilli, M. Crovella, A. Chaintreau, and C. Diot, "Delegation forwarding," in *Proc. ACM Int. Symp. Mobile Ad Hoc Netw. Comput.*, May 2008, pp. 251–260.

[32] A. Lindgren, A. Doria, and O. Schelén, "Probabilistic routing in intermittently connected networks," *ACM SIGMOBILE Mobile Comput. Commun. Rev.*, vol. 7, no. 3, pp. 19–20, Jul. 2003.

[33] T. Spyropoulos, T. Turletti, and K. Obraczka, "Routing in delay-tolerant networks comprising heterogeneous node populations," *IEEE Trans. Mobile Comput.*, vol. 8, no. 8, pp. 1132–1147, Aug. 2009.

[34] M. Chuah, B. Herbst, and D. Li, "Gateway-based interdomain routing scheme for intentional named message delivery in disruption tolerant networks," in *Proc. IEEE Military Commun. Conf. (MILCOM)*, Nov. 2011, pp. 1934–1939.

[35] C. Lee, S. Kang, and K.-I. Kim, "Design of hierarchical routing protocol for heterogeneous airborne ad hoc networks," in *Proc. Int. Conf. Inf. Netw. (ICOIN)*, Feb. 2014, pp. 154–159.

[36] A. Gosavi, "Relative value iteration for average reward semi-Markov control via simulation," in *Proc. IEEE Winter Simulations Conf. (WSC)*, Dec. 2013, pp. 623–630.

[37] J. Clapper, J. Young, J. Cartwright, and J. Grimes, "Unmanned systems roadmap 2007-2032," *Office Secretary Defense*, p. 188, 2007.

WEIJING QI received the M.S. degree in communication and information systems from Northeastern University, Shenyang, China, in 2015, where she is currently pursuing the Ph.D. degree. Her research interests include routing and topology control in space information networks.

WEIGANG HOU received the Ph.D. degree in communication and information systems from Northeastern University, Shenyang, China, in 2013. He is currently an Associate Professor with the School of Computer Science and Engineering, Northeastern University. His research interests include Internet of Things, optical network and traffic grooming, optical network and SDN, optical network and cloud data center, and optical network and chip. He has authored over 70 technical papers in the above areas in inter-national journals and conferences, such as the IEEE Network, the IEEE/OSA Journal of Lightwave Technology, the IEEE/OSA Journal of Optical Communications and Networking, the IEEE GLOBECOM, and the IEEE ICC. He is a member of the OSA.

LEI GUO (M'06) received the Ph.D. degree from the University of Electronic Science and Technology of China in 2006. He is currently a Professor with Northeastern University, Shenyang, China. His research interests include communication networks, optical communications, and wireless communications. He has authored over 200 technical papers in the above areas in international journals and conferences, such as IEEE Transactions on Communications, the IEEE Transactions on Wireless Ccommunications, the IEEE/OSA Journal of Lightwave Technology, IEEE/OSA Journal of Optical Communications and Networking, the IEEE GLOBECOM, and the IEEE ICC. He is a member of the OSA and also a Senior Member of CIC. He is currently serving as an Editor for five international journals, such as *Photonic Network Communications* and *The Open Optics Journal*.

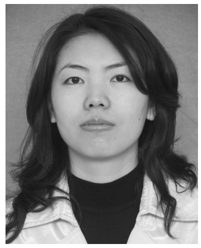

QINGYANG SONG (SM'12) received the Ph.D. degree in telecommunications engineering from The University of Sydney, Australia. She is currently a Professor with Northeastern University, China. She has authored over 50 papers in major journals and international conferences. These papers have been cited over 900 times in scientific literature. Her current research interests are in radio resource management, cognitive radio networks, cooperative communications, ad-hoc networks, heterogeneous cellular networks, and protocol design.

ABBAS JAMALIPOUR (S'86–M'91–SM'00–F'07) received the Ph.D. degree in electrical engineering from Nagoya University, Japan. He is currently a Professor of Ubiquitous Mobile Networking with The University of Sydney, Australia. He has authored six technical books, eleven book chapters, over 450 technical papers, and five patents, all in the area of wireless communications. He is a fellow of the Institute of Electrical, Information, and Communication Engineers and the Institution of Engineers Australia, an ACM Professional Member, and an IEEE Distinguished Lecturer. He is an elected member of the Board of Governors from 2014 to 2016 and the Editor-in-Chief of the Mobile World, the IEEE Vehicular Technology Society. He was a recipient of a number of prestigious awards such as the 2010 IEEE ComSoc Harold Sobol Award, the 2006 IEEE ComSoc Distinguished Contribution to Satellite Communications Award, and the 2006 IEEE ComSoc Best Tutorial Paper Award. He has held positions of the Chair of the Communication Switching and Routing and the Satellite and Space Communications Technical Committees and the Vice Director of the Asia Pacific Board, in ComSoc. He was the General Chair or the Technical Program Chair for a number of conferences, including IEEE ICC, GLOBECOM, WCNC, and PIMRC. He was the Editor-in-Chief of the IEEE Wireless Communications from 2006 to 2008, the Vice President-Conferences from 2012 to 2013, and a member of the Board of Governors of the IEEE Communications Society, and has been an Editor for several journals.